ORNL/TM-2017/305
CRADA/NFE-07-01094

Air-Source Integrated Heat Pump Development – Final Report

Van D. Baxter
C. Keith Rice
Jeffrey D. Munk
Moonis R. Ally
Bo Shen
R. B. “Dutch” Uselton
(Lennox)

July 2017

CRADA final report for CRADA number NFE-07-01094

Approved for public release. Distribution is unlimited.

OAK RIDGE NATIONAL LABORATORY
MANAGED BY UT-BATTELLE FOR THE US DEPARTMENT OF ENERGY

ORNL/TM-2017/305
CRADA/NFE-07-01094

Energy and Transportation Science Division

AIR-SOURCE INTEGRATED HEAT PUMP SYSTEM DEVELOPMENT – FINAL REPORT

ORNL
Van D. Baxter
C. Keith Rice
Jeffrey D. Munk
Moonis R. Ally
Bo Shen

Lennox Industries, Inc.
R. B. "Dutch" Uselton

Date Published: July 2017

Prepared by
OAK RIDGE NATIONAL LABORATORY
Oak Ridge, Tennessee 37831-6283
managed by
UT-BATTELLE, LLC
for the
US DEPARTMENT OF ENERGY
under contract DE-AC05-00OR22725

CONTENTS

LIST OF FIGURES v
LIST OF TABLES vii
LIST OF ACRONYMS ix
ACKNOWLEDGMENTS xi
EXECUTIVE SUMMARY xiii
1. INTRODUCTION 1
2. BACKGROUND—AS-IHP CONCEPT DEVELOPMENT 3
3. FIRST-GENERATION WH/DH PROTOTYPE DESIGN AND SIMULATION APPROACH 8
4. ANNUAL ENERGY USE ANALYSIS AND SAVINGS PREDICTIONS FOR AS-IHP BASED ON FIRST WH/DH PROTOTYPE DESIGN 17
5. SECOND-GENERATION WH/DH PROTOTYPE AND AS-IHP FIELD-TEST SYSTEM DEVELOPMENT 19
6. FIELD-TEST SYSTEM PERFORMANCE AND ANALYSIS 23
7. FURTHER COMMERCIAL PRODUCT DEVELOPMENT PLANS 39
8. CONCLUSIONS 39
9. REFERENCES 40
APPENDIX A. INVENTION DISCLOSURES FILED UNDER CRADA WORK PROGRAM A-1

LIST OF FIGURES

Figure 1. Conceptual installation of residential AS-IHP. 1
Figure 2 AS-IHP system schematic with SC plus “on-demand” WH mode shown. 2
Figure 3. Two-unit AS-IHP concept schematic. 3
Figure 4. Fluted tube-in-tube water-to-refrigerant heat exchanger (Rice et al. 2014). 8
Figure 5. CAD Drawing of prototype WH/DH module layout (Rice et al. 2014). 9
Figure 6. Refrigerant-side design in WH and DH modes (Uselton 2014). 10
Figure 7. WH/DH indoor airflow and condenser subcooling parametrics (Rice et al. 2014). 10
Figure 8. WH/DH module as received with bover removed: (a) compressor; (b) WH mode condenser; (c) DH mode condenser; (d) evaporator; (e) mode switch valve; (f) thermal expansion valve and distributor; (g) water pump; (h) blower housing; and (i) air filter (Rice et al. 2014). 13
Figure 9. Steady-state WH capacity test results showing performance improvement after isolating condenser with insulation (Rice et al. 2014). 15
Figure 10. WH/DH EF test water inlet and outlet temperatures (Rice et al. 2014). 16
Figure 11. Final steady-state WH COP test results—Prototype 1 (Rice et al. 2014). 16
Figure 12. Assumed daily hot water draw schedule from DHW tank (Rice et al. 2014). 17
Figure 13. Second-generation WH/DH module prototype. 19
Figure 14. Second-generation prototype blower performance vs. first-generation blower. 20
Figure 15. Schematic of coaxial tank water fitting. 21
Figure 16. Field-test WH/DH prototype. 21
Figure 17. CAD drawing of field-test prototype WH/DH module. 22
Figure 18. Two-unit AS-IHP field-test system arrangment. 23
Figure 19. Field-test site. 24
Figure 20. Field-test prototype in installation process. ASHP indoor air handler and WH/DH prototype shown with rain gauges for condensate collection (to monitor DH and latent cooling loads). 24
Figure 21. Field data acquisition system. 25
Figure 22. Hot water use control valves. 26
Figure 23. WH/DH cycling between DH mode and V mode with condensate evaporation during ventilation, for equal V and DH airflow rates (top plot) and with reduced airflow during V mode (bottom plot) (Munk et al. 2017). 28
Figure 24. Monthly DH efficiency and runtime (Munk et al, 2017). 28
Figure 25. Histogram of daily hot water use at the research house (Munk et al. 2017). 29
Figure 26. WH mode COP for various entering air and DHW temperatures with percentage of total WH operating hours labeled for each set of conditions (Munk et al. 2017). 30
Figure 27. Monthly average WH mode COPs of the WH/DH HP with and without backup resistance heat use and heat losses from the storage tank and water lines connecting the WH/DH to the storage tank (Munk et al. 2017). 31
Figure 28. Field-test house 2015–2016 heating and cooling load lines 34
Figure 29. Field-test house 2015–2016 heating and cooling load lines vs. AHRI 210/240 load lines (max and min). 34
Figure 30. Average hourly heating, sensible cooling, and latent cooling loads of the field-test house (Munk et al. 2017). 37
Figure 31. Cooling and heating season hours falling within outdoor air temperature bins (Munk et al. 2017). 37

LIST OF TABLES

Table 1. Daily hot water draw schedule assumed for analysis 5
Table 2. Annual SH, SC, WH, and demand DH loads for an nZEH-ready house in five US locations 5
Table 3. Annual site HVAC/WH system energy use and hourly peak demand for an nZEH-ready house with baseline HVAC/WH system 6
Table 4. Estimated annual site HVAC/WH system energy use and hourly peak demand with AS-IHP system (winter humidification active) 6
Table 5. Detailed AS-IHP performance vs. baseline system 7
Table 6. Energy use comparison between Lennox AS-IHP prototype (based on first-generation WH/DH) and baseline one- and two-speed equipment suites 12
Table 7. Inlet air and water conditions for DH and WH steady-state testing of WH/DH unit (Rice et al. 2014) 14
Table 8. Energy use and savings predictions for AS-IHP with reduced flow WH/DH unit configuration (Rice et al. 2014) 18
Table 9. WH load fraction for 2600 ft^2 house used in Table 6 and nZEH-ready house (Table 2) 19
Table 10. Field-test WH/DH prototype unit key components list 22
Table 11. SC data for the ASHP and AS-IHP system including the cooling and heating byproducts of the WH/DH (Munk et al. 2017) 32
Table 12. SH data for the ASHP and AS-IHP system including the cooling and heating byproducts of the WH/DH (Munk et al. 2017) 33
Table 13. Site-measured seasonal SH and SC COPs vs. estimated AHRI 210/240 ratings for ASHP unit used in AS-IHP system 33
Table 14. Average vs. 2015–2016 test site heating and cooling degree days 36
Table 15. Estimated annual energy savings for the AS-IHP relative to baseline equipment – based on bin-hour analysis (Munk et al. 2017) 38
Table 16. AS-IHP system 2015–2016 energy savings vs. estimated baseline system performance at test site ((based on 13 SEER ASHP field tests in 2011–2012) 39

LIST OF ACRONYMS

AHAM	Association of Home Appliance Manufacturers
AHRI	Air-Conditioning, Heating, and Refrigeration Institute
AS-IHP	air-source integrated heat pump
ASHP	air-source heat pump
CFR	Code of Federal Regulations
COP	coefficient of performance
CRADA	Cooperative Research and Development Agreement
DAS	data acquisition system
DB	dry bulb
DH	dehumidifier/dehumidification
DHR	design heating requirement (as defined in AHRI Standard 210/240)
DHW	domestic hot water
DOE/BTO	US Department of Energy Building Technology Office
EER	energy efficiency ratio
EF	energy factor
ESP	external static pressure
EWT	entering water temperature
HPDM	heat pump design model
HPWH	heat pump water heater
HSPF	heating seasonal performance factor
HVAC	heating, ventilation and air conditioning
HX	heat exchanger
nZEH	net-zero energy home
ORNL	Oak Ridge National Laboratory
PV	photovoltaic
RH	relative humidity
SC	space cooling
SEER	seasonal energy efficiency ratio
SH	space heating
TC	thermocouple
V	ventilation
VS	variable speed
WH	water heater/water heating
W/R	water-to-refrigerant
W/W	water-to-water

ACKNOWLEDGMENTS

The authors thank Mr. Dutch Uselton and Mr. Travis Crawford of the Lennox Industries, Inc., project team for their considerable contributions to the Cooperative Research and Development Agreement (CRADA) project and to this report. We express appreciation to our ORNL colleagues Dr. Som Shrestha for technical review of the document, Ms. Kathryn Lord for preparation of the draft manuscript, and Ms. Laurie Varma for technical editing of the manuscript. The authors also thank Mr. Antonio Bouza of the US Department of Energy Building Technology Office for supporting Oak Ridge National Laboratory's CRADA efforts under Contract No. DE-AC05-00OR22725 with UT-Battelle, LLC.

EXECUTIVE SUMMARY

Between October 2007 and September 2017, Oak Ridge National Laboratory (ORNL) and Lennox Industries, Inc. (Lennox) engaged in a Cooperative Research and Development Agreement (CRADA) to develop an air-source integrated heat pump (AS-IHP) system for the US residential market. The Lennox AS-IHP concept consisted of a high-efficiency air-source heat pump (ASHP) for space heating and cooling services and a separate heat pump water heater/dehumidifier (WH/DH) module for domestic water heating and dehumidification (DH) services. A key feature of this system approach with the separate WH/DH is capability to pretreat (i.e., dehumidify) ventilation air and dedicated whole-house DH independent of the ASHP. Two generations of laboratory prototype WH/DH units were designed, fabricated, and lab tested. Performance maps for the system were developed using the latest research version of the US Department of Energy/ORNL heat pump design model (Rice 1992; Rice and Jackson 2005; Shen et al. 2012) as calibrated against the lab test data. These maps served as the input to TRNSYS (Solar Energy Laboratory et al. 2010) to predict annual performance relative to a baseline suite of equipment meeting minimum efficiency standards in effect in 2006 (i.e., a combination of an ASHP with a seasonal energy efficiency ratio (SEER) of 13 and resistance water heater with an energy factor (EF) of 0.9). Predicted total annual energy savings (based on use of a two-speed ASHP and the second-generation WH/DH prototype for the AS-IHP), while providing space conditioning, water heating, and dehumidification for a tight, well-insulated 2600 ft^2 (242 m^2) house at three US locations, ranged from 33 to 36%, averaging 35%, relative to the baseline system. The lowest savings were seen at the cold-climate Chicago location. Predicted energy use for water heating was reduced by about 50 to 60% relative to a resistance WH.

Based on the lab prototype tests and analyses results, a field-test prototype WH/DH was designed and fabricated by Lennox. The WH/DH prototype and a variable-speed ASHP were installed in a 2400 ft^2 (223 m^2) research house in Knoxville, Tennessee, and field tested from August 2015 to October 2016. Additional field testing of the WH/DH unit continued through May 2017 to evaluate several design changes intended to improve the DH performance. For the 2015–2016 AS-IHP system test period, overall space conditioning efficiencies were 4.72 for space cooling (SC) and 2.23 for space heating (SH). For water heating (WH), the overall average coefficient of performance (COP) was 2.75 for the WH/DH unit only and 2.19 for the total system, including COP degradations due to heat losses from the connecting lines between the WH/DH and tank (~10%), heat losses from the water tank (~8%), and backup electric heat usage (~3%). The WH COP was also negatively impacted by a 20-day period in January 2016 during which there were no hot water draws due to a control issue. Overall, the field demonstrated DH efficiency (when examining only the months with significant run hours in DH mode) was 1.7 L/kWh; monthly averages ranged from 1.5 to 2.1.

Based on the demonstrated field performance of the AS-IHP prototype and estimated performance of a baseline system operating under the same loads and weather conditions, a bin analysis estimated that the prototype would achieve ~30% energy savings relative to the minimum efficiency suite. The estimated WH savings were ~60%, and SC mode savings were >30%. However, estimated SH savings were only about 10%. We found that the heating load for the field-test house was about 50% higher at the 5°F design condition than that used for heating seasonal performance factor ratings calculations for this size unit. This resulted in a higher level of use of backup electric resistance heating (at a COP of 1) than would be assumed for the ratings calculations. Issues were also found with the zone control system, which penalized the space conditioning (particularly the space cooling) performance of the variable speed ASHP. A secondary comparison based on earlier field tests of two baseline 13 SEER ASHPs in another house in the same area with lower heating loads indicated ~40% overall energy savings for the AS-IHP: ~60% WH savings, ~45% SC savings, and ~25% SH savings.

1. INTRODUCTION

Oak Ridge National Laboratory (ORNL), UT-Battelle, LLC, and Lennox Industries, Inc. (Lennox) initiated a Cooperative Research and Development Agreement (CRADA) to support development of a new residential heating, ventilation and air conditioning (HVAC) & water heating (WH) product—an air-source integrated heat pump (AS-IHP). The goal was to introduce a new, highly efficient class of products for providing energy services (e.g., space heating and cooling [SH/SC], WH, and indoor humidity control) to residential and small commercial buildings while consuming ~50% less energy than current minimum efficiency equipment. This project was one of two similar CRADA projects devoted to AS-IHP prototype system development. The other was conducted in partnership with Nordyne, LLC, and has been summarized in a report by Baxter et al. (2015).

The US Department of Energy's Building Technologies Office (DOE-BTO) has a long-term goal to reduce the energy use intensity of US buildings by 30% vs. 2010 levels by 2030, increasing to 50% in the long term (Risser 2016). To achieve this vision, a deep reduction of the energy used by the energy service equipment providing SH/SC, WH, and indoor humidity control is required—50% compared with today's best common practice. One approach to achieving this is to produce a single system that provides multiple services. In FY05–07 ORNL developed a general concept for such an appliance, the IHP. Figure 1 illustrates conceptual installation, and Figure 2 provides a schematic drawing (Murphy et al. 2007). Figure 2 illustrates a major energy-saving feature of the IHP concept: combined SC and WH operation wherein heat normally rejected in SC is recovered for WH (i.e., the SC plus "on demand" WH mode).

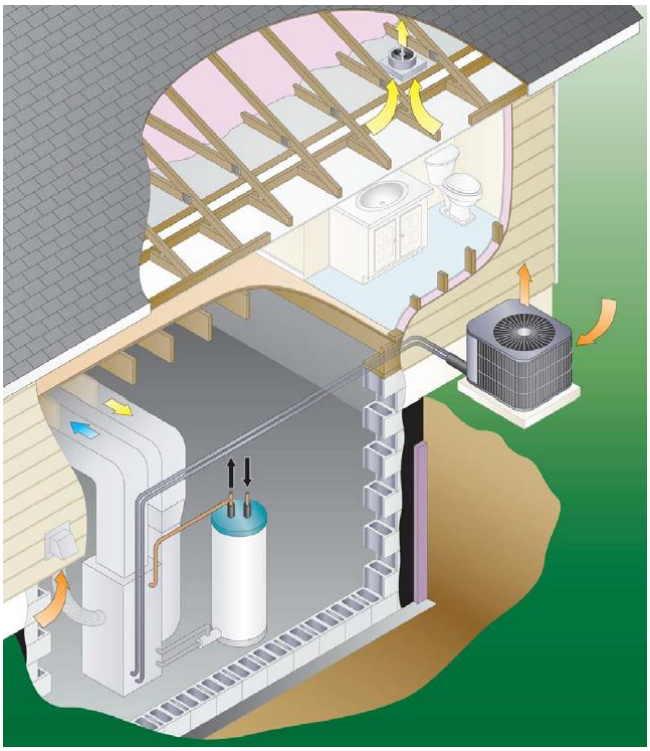

Figure 1. Conceptual installation of residential AS-IHP.

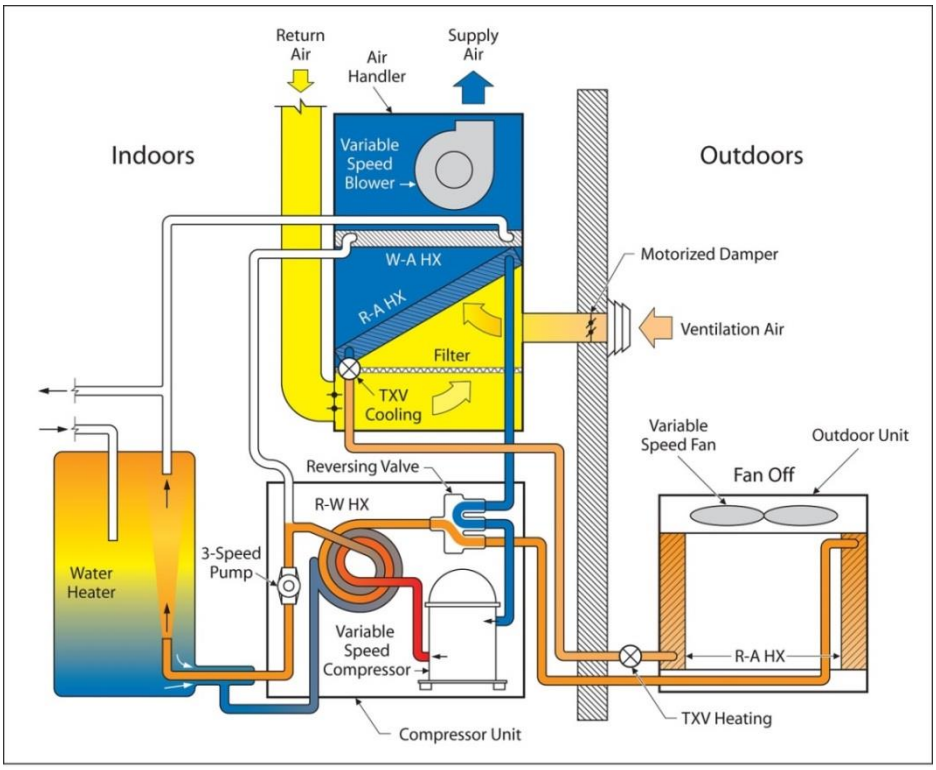

Figure 2 AS-IHP system schematic with SC plus "on-demand" WH mode shown.

Successful achievement of program goals requires that DOE not only develop the IHP concept, but also facilitate introduction of such equipment to the US building market. For this activity to have the best chance of success, collaboration with manufacturing partners with experience in developing and marketing HVAC products is critical. Lennox expressed interest in the AS-IHP concept and agreed to partner with ORNL in this CRADA.

Lennox's specific embodiment of the IHP concept (Uselton 2012, 2014) is a variable-capacity, "two-unit" or "two-compressor" system in contrast to the single-compressor approach utilized in the original ORNL concept. This IHP system concept combines a high-efficiency air-source heat pump (ASHP) already marketed by Lennox to provide SH/SC together with a separate prototype equipment module for WH and demand dehumidification (DH) services—a WH/DH module. Figure 3 provides a schematic of the concept. The WH/DH module is integrated with the central heat pump unit by a parallel secondary duct loop around the central air handler, receiving a portion of the central return air when the secondary (WH/DH) blower is operating and returning this air to the supply side. It also has an optional connection to an outdoor air intake to provide a means for preconditioning and circulating ventilation (V) air through the central duct system.

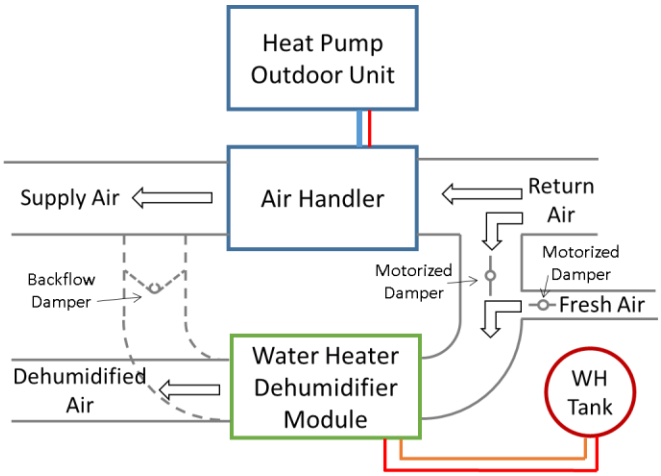

Figure 3. Two-unit AS-IHP concept schematic.

One motivation for this unusual equipment combination is the trend toward increasingly efficient thermal envelopes for new homes leading to lower sensible SC loads and, subsequently, lower sensible heat ratios of the building's SC loads. Homes with tighter, more energy-efficient thermal envelopes have lower sensible loads and greatly reduced incidental outdoor air infiltration, but internal moisture loads from occupants, showers, laundry, and cooking can become a problem. At the same time, tighter envelopes may impose a need for mechanical ventilation to maintain acceptable internal air quality. Humidity in some areas of the US and other countries will further exacerbate internal moisture loads. A dedicated space DH cycle addresses humidity control, and integration of heat pump WH is expedient since the small vapor compression components can perform double duty. The integrated yet independent operation of the WH/DH unit provides dedicated DH of the central return and outdoor ventilation air as well as a central heat source for the WH mode. The independent operation is especially useful during the shoulder months, when WH loads and, in many cases DH loads, exist but sensible SC and SH loads are small.

Another significant motivation is that this approach can be much more easily applied to retrofit or upgrade applications, utilizing standard electric water heaters and a wide range of multi-capacity and variable speed (VS) ASHPs. Where an existing home WH tank is remote from the ASHP system, the WH/DH unit can be co-located with the WH tank. This may mean that connecting the WH/DH to the central ASHP return duct system may not be possible, but most of the benefits of the IHP concept will still be retained.

Project tasks were undertaken to design several WH/DH module prototypes, produce lab test systems, refine the design, and produce a prototype for field testing.

2. BACKGROUND—AS-IHP CONCEPT DEVELOPMENT

Full details of the AS-IHP concept development can be found in Murphy et al. (2007) and are briefly summarized here to provide context for system development activities under the CRADA. This system concept (Figure 2) uses one VS modulating compressor; a VS indoor blower and outdoor fan; and a multispeed pump for hot water circulation, including a 50-gallon (~189 L) WH tank. The original concept included a dedicated DH mode and a humidifier option. The concept analyses were based on a relatively small (1800 ft^2 or 167 m^2) and very-well-insulated house with nominal space cooling design loads of 1–1.5 tons (3.5–5.3 kW) depending upon location (e.g., insulation and SH/ SC load levels needed to reach net-zero energy home [nZEH] performance). The Lennox system is based on use of a 2–3 ton (~7.0–10.5

kW) nominal size ASHP designed for somewhat larger residences typical of new construction practice. For such homes, the fraction of the total load due to WH is reduced from the original concept.

Annual energy use simulations for a baseline suite of individual systems and the AS-IHP were performed using the TRNSYS16 platform. The baseline suite consisted of a 13 SEER/7.7 HSPF ASHP, 0.90 energy factor (EF) electric WH, standalone dehumidifier representative of average units available in 2006, the humidifier option, and ventilation per American Society of Heating, Refrigerating and Air-Conditioning Engineers (ASHRAE) standard 62.2 (ASHRAE 2007) requirements. Annual subhourly simulations were performed for the baseline system and the IHP in an 1800 ft^2, NZE-ready house for five locations:

- Atlanta (mixed–humid climate)
- Houston (hot–humid climate)
- Phoenix (hot–dry climate)
- San Francisco (marine climate)
- Chicago (cold climate)

The relatively small house coupled with its NZE-ready insulation characteristics resulted in very low cooling design loads and nominal IHP cooling capacity levels. Simulating the IHP systems required that the ORNL heat pump design model (HPDM) be utilized to develop detailed performance maps for each operating mode, which were then input to TRNSYS. Set points for space heating and cooling were 71 °F and 76 °F (21.7 °C and 24.4 °C), respectively. The WH set point was 120 °F (48.9 °C) and total daily hot water use of ~64.5 gallons (~245 L) was assumed using the schedule shown in Table 1. The systems' humidity control set points (i.e., dehumidifier and humidifier for the baseline; dedicated dehumidification mode and humidifier for the IHP) were set to maintain indoor relative humidity (RH) of ≤60% in summer, fall, and spring and ≥30% in winter.

Table 1. Daily hot water draw schedule assumed for analysis

Event	Start time (h)	Duration (min)	Fraction of daily consumption
Shower	a.m. 6:00	12	0.172
Shower	6:15	12	0.172
Shower	6:30	12	0.172
Lavatory	6:00	1	0.014
Lavatory	6:15	1	0.014
Kitchen sink	6:45	2	0.029
Kitchen sink	7:30	2	0.029
Clothes wash cycle	9:00	3	0.204
Lavatory	p.m. 12:15	1	0.014
Kitchen sink	12:30	1	0.014
Lavatory	4:45	1	0.014
Lavatory	5:15	1	0.014
Dishwasher (1st wash)	7:30	1.5	0.048
Dishwasher (2nd wash)	8:00	1.5	0.048
Lavatory	9:45	1	0.014
Lavatory	10:15	1	0.014
Lavatory	10:30	1	0.014

Table 2 shows the annual loads for the nZEH-ready house obtained from the TRNSYS simulations reported by Murphy et al. (2007) for the five US climate locations. It also shows the nominal design SC capacity necessary for each city and the fraction of the total IHP system load, excluding the demand DH loads) due to WH.

Table 2. Annual SH, SC, WH, and demand DH loads for an nZEH-ready house in five US locations

Location	Space heating load (kWh)	Space cooling load (kWh)	Water heating load (kWh) (% of total SH+SC+WH load)	Demand dehumidification load (kWh)	Heat pump design SC capacity (kW) tons)
Atlanta	4775	5735	3032 (22)	158	4.40 (1.25)
Houston	1766	9927	2505 (18)	704	4.40 (1.25)
Phoenix	1580	9759	2189 (16)	-	5.28 (1.50)
San Francisco	2881	88	3387 (53)	42	3.52 (1.00)
Chicago	11475	2550	3807 (21)	94	4.40 (1.25)

Table 3 provides summary results from annual performance simulations for the baseline HVAC system for the five locations. Table 4 provides the annual results for the AS-IHP including hourly integrated peak demand. For both systems, maximum peaks generally occurred in the winter. Summer peaks are

somewhat lower and generally occurred in July or August. Detailed results from the simulations are given in Table 5. The total energy consumption and consumption by individual modes for the baseline system are from the TRNSYS simulations. For the AS-IHP, the total energy consumption, for the ventilation fan and electric backup WH and SH, are from the detailed TRNSYS simulations. Breakdowns for the other AS-IHP modes were taken from the hourly simulations as well, but with adjustments to fairly charge the water pump power in combined modes to the WH function.

Table 3. Annual site HVAC/WH system energy use and hourly peak demand for an nZEH-ready house with baseline HVAC/WH system

Location	Heat pump cooling capacity (kW) (tons)	Site energy use (kWh)	Hourly peak kW demand (W/S/SA)*
Atlanta	4.40 (1.25)	7230	8.6/4.6/2.1
Houston	4.40 (1.25)	7380	6.1/4.4/2.2
Phoenix	5.28 (1.50)	6518	6.1/3.9/2.1
San Francisco	3.52 (1.00)	4968	5.7/5.6/1.6
Chicago	4.40 (1.25)	10773	9.7/6.1/2.4

* W–winter morning; S–summer maximum; SA–summer midafternoon.

Table 4. Estimated annual site HVAC/WH system energy use and hourly peak demand with AS-IHP system (winter humidification active)

Location	Heat pump cooling capacity (tons)	Site energy use (kWh)	Hourly peak kW demand (W/S/SA)*	% energy savings vs. baseline HVAC
Atlanta	4.40 (1.25)	3349	2.2/1.5/1.2	53.7
Houston	4.40 (1.25)	3418	1.9/1.1/1.1	53.7
Phoenix	5.28 (1.50)	3361	2.1/1.7/1.7	48.4
San Francisco	3.52 (1.00)	1629	1.8/1.6/0.8	67.2
Chicago	4.40 (1.25)	5865	7.3/1.6/1.0	45.6

* W–winter morning; S–summer maximum; SA–summer midafternoon.

The results summarized in Tables 4 and 5 show that the AS-IHP exceeded 50% savings over the baseline system in three of the five locations, almost reaching 70% in the mild San Francisco climate. The summer cooling performance of the concept system design under the extreme hot outdoor conditions seen in Phoenix is not quite high enough to enable reaching 50% annual savings in this SC-dominated climate. In Chicago, the energy service loads are dominated by heating—SH and WH together constitute ~84% of the total load—and the AS-IHP heating performance declines during the extremely cold temperatures encountered in this climate.

Winter peak demand was approximately 25 to 75% lower for the AS-IHPs than for the baseline. Maximum summer peaks usually occurred in the morning during peak domestic hot water (DHW) demand periods and were about 55 to 75% lower vs. the baseline. Summer midafternoon peaks were ~20 to 60% lower than those of the base system, depending upon location.

Table 5. Detailed AS-IHP performance vs. baseline system

Loads (1800 ft^2 highly efficient house from TRNSYS)		Equipment		
		Baseline	AS-IHP	
Source	kWh	Energy use (kWh) (I^2R)*	Energy use (kWh) (I^2R)	Energy reduction compared to baseline
Atlanta				
Space Heating	4775	1789 (51)*	1251	30.1%
Space Cooling	5735	1643	1073	34.7%
Water Heating	3032	3402	924 (142)	72.8%
Dedicated DH	158	208	82	60.4%
Ventilation fan	–	189	20	89.6%
Totals	13,701	7230	3349	**53.7%**
Humidifier water use	499 kg		618 kg	
Houston				
Space Heating	1766	648	474	26.9%
Space Cooling	9927	2853	1894	33.6%
Water Heating	2505	2816	556 (91)	80.2%
Dedicated DH	704	875	482	44.9%
Ventilation fan	–	189	12	93.7%
Totals	14,902	7380	3418	**53.7%**
Humidifier water use	75 kg		87 kg	
Phoenix				
Space Heating	1580	535	336	37.1%
Space Cooling	9759	3317	2296	30.8%
Water Heating	2189	2477	696 (19)	71.9%
Dedicated DH	–	–	–	na
Ventilation fan	–	189	33	82.7%
Totals	13,527	6518	3361	**48.4%**
Humidifier water use	170 kg		229 kg	
San Francisco				
Space Heating	2881	932	607	34.8%
Space Cooling	88	26	23	12.5%
Water Heating	3387	3767	957 (100)	74.6%
Dedicated DH	42	54	11	80.3%
Ventilation fan	–	189	32	83.2%
Totals	6398	4968	1629	**67.2%**
Humidifier water use	34 kg		38 kg	
Chicago				
Space Heating	11,425	5448 (1415)	3686 (614)	32.3%
Space Cooling	2550	729	436	40.1%
Water Heating	3807	4286	1644 (327)	61.6%
Dedicated DH	94	121	83	31.9%
Ventilation fan	–	189	17	91.1%
Totals	17,877	10,773	5865	**45.6%**
Humidifier water use	1369 kg		1639 kg	

*(I^2R) and numbers in red indicate SH and WH energy consumption due to backup electric resistance elements.

3. FIRST-GENERATION WH/DH PROTOTYPE DESIGN AND SIMULATION APPROACH

The AS-IHP concept investigation summarized above led to collaboration with Lennox aimed at developing a design suitable for residential applications typical of current construction practices. Much of the information presented in this and the next three sections are taken from two papers: Rice et al. (2014) and Munk et al. (2017).

WH/DH prototype design goals and analyses.

Design performance goals for the WH/DH unit are to meet or exceed Energy Star performance levels for WH and DH modes of operation. For the DH mode, the EF requirement for Energy Star rating from October 1, 2012 through October 24, 2016 (Energy Star 2012) was ≥1.85 L/kWh for units with DH capacity of <75 pints/day (1.48 L/h) [after October 25, 2016, the EF requirement was increased to ≥2.00 (Energy Star 2016)]. Note that the DH EF values noted here are based on standard indoor ambient conditions of 60% RH and 80 °F temperature. This capacity was determined adequate for the homes and climate locations analyzed for this AS-IHP approach, including those locations with the highest DH loads: Atlanta, Chicago, and Houston. For the WH mode, an EF of ≥2.0 (W/W) is required for Energy Star designation for electric water heaters (Energy Star 2013, 2015). The remaining design goal was to provide WH capacity of ~2 kW, about twice that for standalone residential heat pump water heaters (HPWHs).

A prototype design suitable for lab testing was assembled by Lennox, starting from a whole-house dehumidifier unit. The prototype uses an R-410A rotary compressor rated at about 7000 Btu/h (2 kW) and 9.5 Btu/Wh energy efficiency ratio (EER) (COP of 2.8) under air-conditioning conditions. Separate condensers are used for each operating mode—a 1-ton (3.5 kW) fluted tube-in-tube double-walled water-to-refrigerant (W/R) heat exchanger (HX) and a three-row fin-and-tube air-to-refrigerant HX, in combination with a common two-row fin-and-tube evaporator. Figure 4 shows the tube-in-tube HX unit and a cutaway of the fluted tube design, where water flows through the inner fluted tube and refrigerant flows through the fluted annulus. This HX was installed around the rotary compressor as can be seen in the CAD drawing of Figure 5.

Figure 4. Fluted tube-in-tube water-to-refrigerant heat exchanger (Rice et al. 2014).

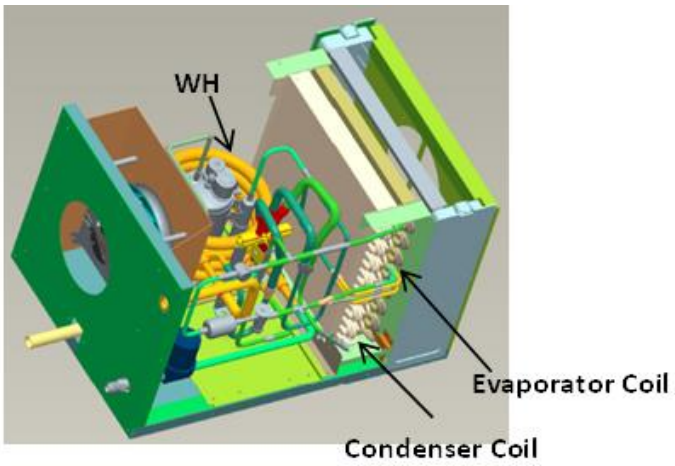

Figure 5. CAD Drawing of prototype WH/DH module layout (Rice et al. 2014).

Refrigerant-side schematics of the design in the two operating modes are shown in Figure 6 (Uselton 2014). The switchover valve shown in the drawing is used to switch active condensers between modes; the inactive suction port side is also used as a vent to return refrigerant from the inactive condenser. A thermostatic expansion valve is used to regulate refrigerant flow based upon evaporator superheat. A draw-through backward-curved centrifugal blower and high-efficiency water pump, both with VS brushless permanent magnet motors, completes the major components list.

The HPDM was used in two setup configurations to model the prototype design and determine predicted optimal refrigerant, air, and water control settings for the two operating modes. The fluted-tube W/R model in the HPDM requires internal geometry specifications obtained by direct measurements of the cutaway section shown in Figure 4. The refrigerant-side volume and other volume-related geometry information were first obtained by successively filling the inner tube and annulus with water and comparing the weight of the assembly with that of an empty HX. Details of the air-to-refrigerant HXs as well as compressor, blower, and pump performance maps were provided by their respective manufacturers. Lennox's initial WH/DH prototype test data were used in conjunction with the HPDM to predict the optimal refrigerant subcooling levels and air and water flows at the selected design conditions, which were entering air conditions of 80 °F (26.7 °C)/60% RH for DH and 67.5 °F (19.7 °C)/50% RH for the WH with a 108 °F (42.2 °C) entering water temperature. The water flow for the WH mode was set at the maximum available flow of 2.3 gpm (0.145 L/s) for an expected static pressure head curve.

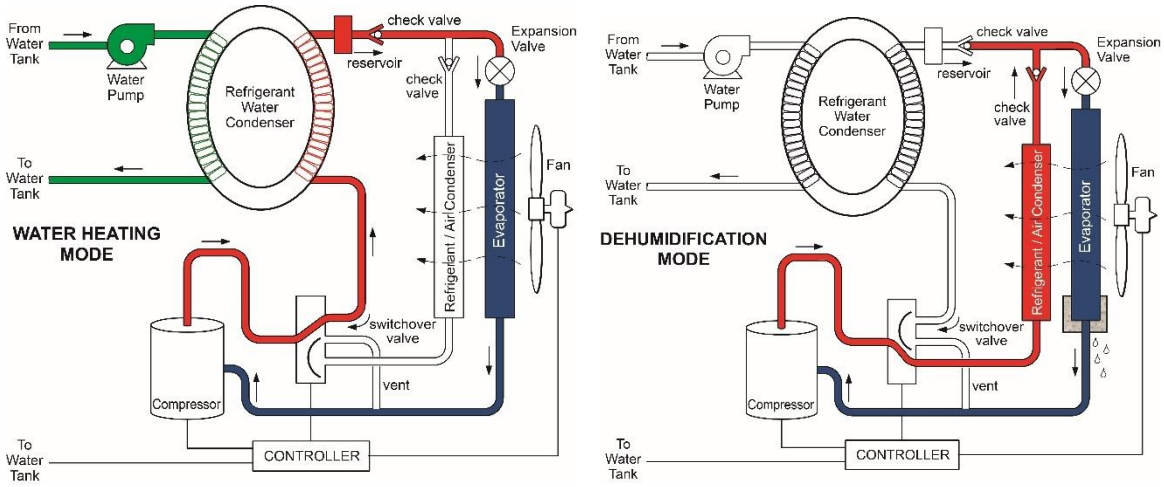

Top: WH mode **Bottom: DH mode**

Figure 6. Refrigerant-side design in WH and DH modes (Uselton 2014).

For the WH mode, the optimum COP was approximately 10 °F (5.6 °C) subcooling and 300 cfm (142 L/s), as shown in Figure 7a by the bold **X**. For the DH mode, the design goal of <75 pints/day (1.48 L/h) and Energy Star efficiency could be achieved with the same subcooling and airflow as denoted in Figure 7b by the bold **X**. This design subcooling level and related charge quantity, lower than for a typical DH design, was a compromise made to ensure compatibility with efficient operation in WH mode.

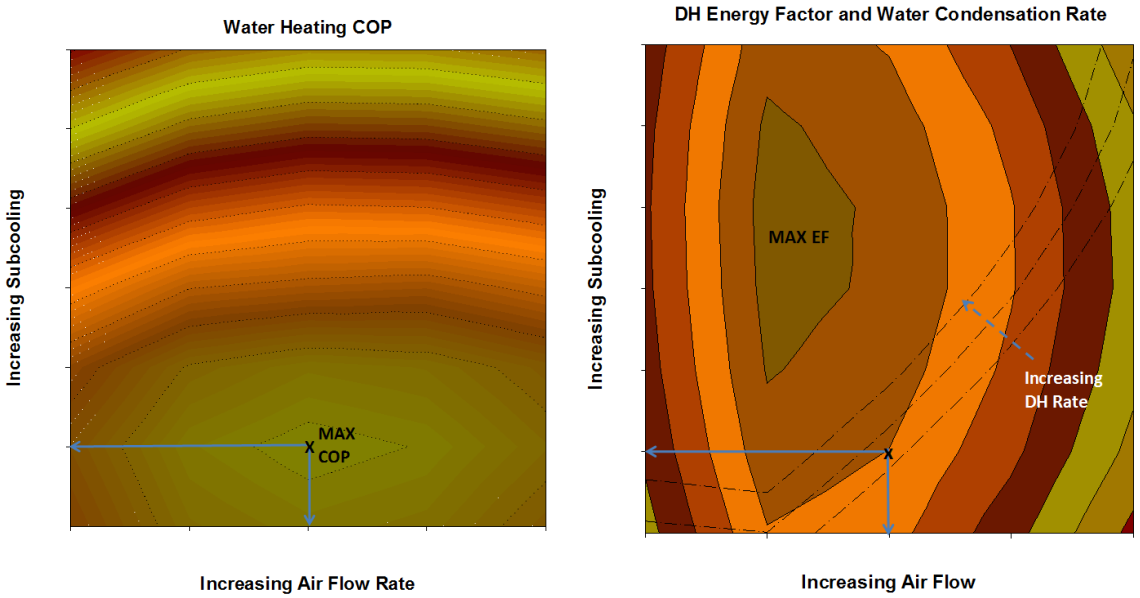

(a) WH mode **(b) DH mode**

Figure 7. WH/DH indoor airflow and condenser subcooling parametrics (Rice et al. 2014).

Preliminary AS-IHP energy savings estimates based on first- generation WH/DH prototype design.

Using test data provided by Lennox for their 2-ton, two-speed ASHP (SEER of 18.4 and HSPF of 9.1) (Lennox 2009a, 2009b), and the prototype WH/DH, the team developed calibrated HPDM models for

each operational configuration. Available design parameters such as air and water flow rates and refrigerant charge were optimized for the DH and WH modes. Initial control logic was provided by Lennox, and this was refined during setup and testing of the TRNSYS simulations to allow independent operation of the DH or WH modes, as appropriate, along with the primary space conditioning modes.

Bottom-line results (Table 6) show estimated energy savings for an AS-IHP design based on the selected ASHP. The first WH/DH prototype ranged from just over 36% for Chicago to almost 39% for Atlanta and Houston. These savings are relative to the primary baseline suite of an R-410A ASHP (SEER of 13, HSPF of 7.7); standalone dehumidifier (DH EF of 1.4); and 0.9 EF electric resistance WH in a 2600 ft^2 (242 m^2) nZEH-ready house. WH-only savings range from ~56 to 60% (average annual WH COP of ~2.1–2.2). The second baseline included in the table replaces the minimum-efficiency ASHP with two-speed Lennox unit with the same DH, WH, and ventilation options. By comparing the energy use in SH/SC with that of the integrated approach, one can see the increase in SH energy use and the decrease in SC use caused by the WH system's cooling of the air, the relative sizes of which vary by climate. Note also that the DH energy use for the AS-IHP prototype is 28% less than for the baseline cases.

Table 6. Energy use comparison between Lennox AS-IHP prototype (based on first-generation WH/DH) and baseline one- and two-speed equipment suites

Loads & Energy Use by Mode - 2-Ton 410A Baseline 13 SEER Heat Pump vs. 2spd ASHPs; 2600 ft^2 ZEH								
Loads (from baseline simulation)		Equipment						
		Baseline	2-Speed ASHP w I2R WH, Standalone DH			2-Speed ASHP + DH/WH/Vent unit		
mode	kWh	energy use, kWh (I^2R)	energy use, kWh (I^2R)	% red from base	case notes	energy use, kWh (I^2R)	% red from base	case notes
Atlanta								
space heating	5996	2311	1601	30.7%	Baseline Lennox 2-speed ASHP; same I^2R WH, standalone DH, central AirCycler circulation, and continuous bathroom exhaust vent as baseline 1-speed ASHP	1857	19.6%	Lennox 2-speed ASHP integrated with DH/WH/Vent Unit
resistance heat		(18)	(0)			(2)		
space cooling	6267	1741	1179	32.3%		1083	37.8%	
water heating	3032	3380	3380	0.0%		1421	58.0%	
resistance heat		(3380)	(3380)			(154)		
dedicated DH	239	319	454	-42.4%		228	28.6%	
ventilation fan		189	189	0.0%		290	-53.5%	
totals	15534	7941	6804	14.3%		4880	38.6%	
Houston								
space heating	2672	995	705	29.2%	Baseline Lennox 2-speed ASHP; same I^2R WH, standalone DH, central AirCycler circulation, and continuous bathroom exhaust vent as baseline 1-speed ASHP	857	13.9%	Lennox 2-speed ASHP integrated with DH/WH/Vent Unit
resistance heat		(0)	(0)			(0)		
space cooling	10830	3035	2152	29.1%		1947	35.8%	
water heating	2505	2813	2813	0.0%		1122	60.1%	
resistance heat		(2813)	(2813)			(57)		
dedicated DH	911	1154	1418	-22.8%		822	28.8%	
ventilation fan		189	189	0.0%		272	-43.6%	
totals	16918	8187	7277	11.1%		5020	38.7%	
Chicago								
space heating	13370	6214	4172	32.9%	Baseline Lennox 2-speed ASHP; same I^2R WH, standalone DH, central AirCycler circulation, and continuous bathroom exhaust vent as baseline 1-speed ASHP	4709	24.2%	Lennox 2-speed ASHP integrated with DH/WH/Vent Unit
resistance heat		(916)	(455)			(554)		
space cooling	2660	740	512	30.8%		421	43.0%	
water heating	3807	4218	4218	0.0%		1838	56.4%	
resistance heat		(4218)	(4218)			(314)		
dedicated DH	117	154	222	-44.5%		129	16.2%	
ventilation fan		189	189	0.0%		254	-34.1%	
totals	19955	11514	9314	19.1%		7351	36.2%	

WH/DH first-generation prototype detailed lab test results.

Following in-situ blower and operational unit testing, Lennox shipped the prototype WH/DH module to ORNL for detailed laboratory testing and performance mapping. Figure 8 provides a photo of the unit with covers removed to show the interior component arrangement.

The WH/DH unit was tested in a small environmental chamber along with a nominal 50-gal (190 L) water tank (with actual volume of 9% less) connected by insulated water hoses. Unit inlet RH was measured using an RH transducer with the inlet dry-bulb (DB) temperature obtained from a four-point averaging Type-T thermocouple (TC) grid. The WH/DH airflow rate was not measured directly; it was controlled to ~300 cfm (142 L/s) under wet coil conditions based on fan external static pressure drop data obtained from in-situ fan tests conducted by Lennox. A short length of round duct with an adjustable damper was installed upstream to regulate the external static pressure head on the WH/DH blower.

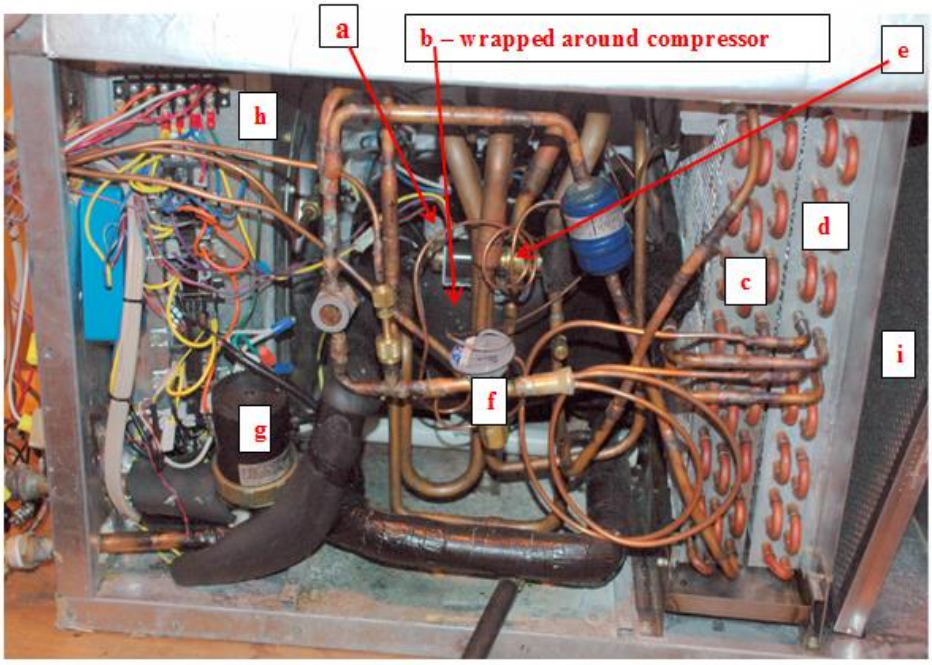

Figure 8. WH/DH module as received with cover removed: (a) compressor; (b) WH mode condenser; (c) DH mode condenser; (d) evaporator; (e) mode switch valve; (f) thermal expansion valve and distributor; (g) water pump; (h) blower housing; and (i) air filter (Rice et al. 2014).

Note, however, that the measurements of the WH and DH capacities are not dependent on knowledge of the airflow rate. To determine DH capacity, the condensate collected for the duration of each test period was weighed using an electronic balance scale. Water flow was measured with a turbine flow meter installed in the WH/DH entering water line, with 5 straight pipe diameters upstream and downstream of the meter. Water flow was controlled to ~2.1 gpm (0.132 L/s), the maximum obtainable in the test loop. Refrigerant and water line temperatures were measured with Type-T TCs, all surface mounted and insulated except for the tank water temperatures, which were obtained with immersion TCs. Refrigerant pressures were measured with transducers on the compressor suction, discharge, and liquid line lines, with ranges of 0–250 psia (0–1.72 MPa) on the low side and 0–750 psia (0–5.17 MPa) on the high side. Refrigerant flow rate was calculated from the manufacturer's compressor map using the measured suction and discharge pressures and the suction superheat.

A steady-state test matrix was developed for WH and DH performance mapping tests over a range of inlet air conditions and water temperatures. As indicated in Table 7, for the DH mode, three ambient temperatures and three RHs were used, giving nine test points to span the range of expected return air conditions. In the WH mode, twelve test points were run, using the three most likely indoor DB/RH conditions in combinations with four entering water temperatures (EWTs).

The steady-state WH and DH tests were run for a minimum of 30 minutes and 1 hour, respectively. In addition to the performance mapping, tests were conducted to estimate the EF (24-h duration) and first-hour ratings for the WH mode and the EF rating (6-h duration) for the DH mode using the standard rating test procedures for each mode (US Code of Federal Regulations [CFR] 2010, for WH; Association of Home Appliance Manufacturers [AHAM] 2008, for DH).

Table 7. Inlet air and water conditions for DH and WH steady-state testing of WH/DH unit (Rice et al. 2014)

Test Matrix for DH Mode			Test Matrix for WH Mode			
Test #	Test Condition		Test #	Test Condition		
	Inlet DB, °C	RH %		Inlet DB, °C	RH %	EWT °C
1	26.7	60	1	20.0	50	21.1
2	26.7	55	2	20.0	50	32.2
3	26.7	50	3	20.0	50	43.3
4	23.3	55	4	20.0	50	54.4
5	23.3	60	5	23.3	55	21.1
6	23.3	50	6	23.3	55	32.2
7	20.0	60	7	23.3	55	43.3
8	20.0	55	8	23.3	55	54.4
9	20.0	50	9	26.7	60	21.1
			10	26.7	60	32.2
			11	26.7	60	43.3
			12	26.7	60	54.4

Steady-state DH tests were conducted first to establish the required design charge at DH rating conditions and ~10°F condenser subcooling and to determine the DH capacity. After determining the refrigerant charge needed to achieve the desired superheat and subcooling control, a 6-hour DH standard rating test was run. This confirmed that the capacity was just below the 75 pints/day (1.48 L/h) target with an EF above 2, exceeding the 2012 and 2016 Energy Star minimums for this size dehumidifier. The condensate amount was recorded at the end of each hour of the test, which provided hourly measurements with a maximum deviation of 3.5%. Following this, 1-h steady-state tests were run for each of the nine inlet air condition combinations in Table 1.

Initial steady-state WH tests followed using the same refrigerant charge as for the DH testing. These test results showed somewhat lower WH capacities and COPs than predicted from the simulation. From the refrigerant- and water-side energy flows, the team determined that, for the higher EWTs, there was significant heat loss from the refrigerant in the outer annulus of the WH condenser HX to the cool air stream leaving the evaporator.

Next, a baseline WH mode EF for the "as received" unit was obtained based on the standard 24-h use test procedure in effect prior to April 2015 (US CFR 2010); a value of ~1.5 (lower than expected) indicated that the heat losses within the unit were significant. To minimize heat losses and improve WH

performance, further insulation was added to better insulate and isolate the WH condenser and the compressor from the exiting cold air stream leaving the evaporator.

After these changes, a new set of steady-state WH data was taken and compared with earlier results, as shown in Figure 9. This shows capacity as a function of EWT for three different inlet air conditions. From the capacity plot, isolation of the WH condenser and compressor from the exit air stream significantly boosts the delivered capacity at the higher EWTs as compared with the initial tests (marked "Non" in the legends).

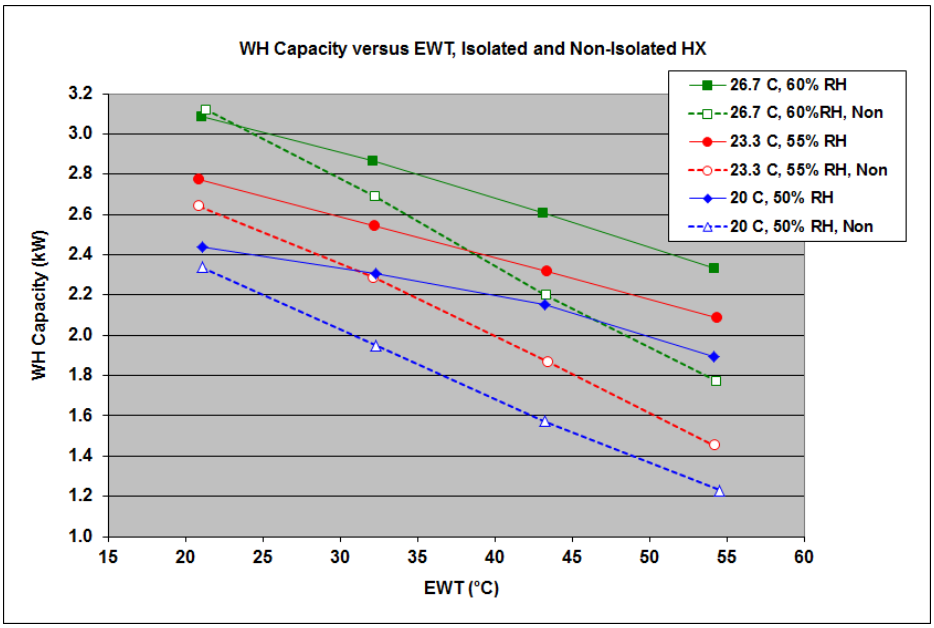

Figure 9. Steady-state WH capacity test results showing performance improvement after isolating condenser with insulation (Rice et al. 2014).

The WH mode EF test was then repeated, this time with a lower WH thermostat setting to keep the maximum tank water temperature from exceeding 135 °F (56.7 °C) as was the case in the first tests. The new EF results improved to ~1.65 but EF was still well below the 2.0 target. Additional insulation was applied to the condenser and compressor along with extra insulation on the refrigerant and water lines inside the unit. A new 24-h use (EF) test followed with a resultant EF of 1.78, an increase of 7.8% from the previous test, but EF was still short of the target level.

Next, from close examination of the tank inlet and exit temperatures during the tank cool-down period, three apparent thermosiphon events were identified in which water that had cooled in the WH-mode condenser flowed back into the bottom of the tank, displacing warmer water in the top of the tank into the WH/DH unit. Note in Figure 10 the three or four events during which the WH water inlet temperature jumped sharply during the standby period after the sixth water draw of the 24-h test.

On discovering this, the team ran a new cool-down test with the water inlet valve closed to prevent the thermosiphon action. From this it was determined that reducing this recurrent heat loss would eliminate the need for any WH/DH unit operation for tank reheat during the standby period of the 24-h EF test and estimated that the resultant EF would have been ~1.9. The WH EF test was repeated after making this adjustment, manually closing the valve in the inlet water line to prevent any thermosiphon incidents. The resultant EF was found to be 1.92, ~8% higher than that of the previous test—much closer to but still short of the target. In summary, the EF was increased from 1.5 to 1.92 over the course of the testing, for a

28% increase. WH mode first-hour recovery rating tests were also run, achieving an acceptable 59 gal (223 L) delivered.

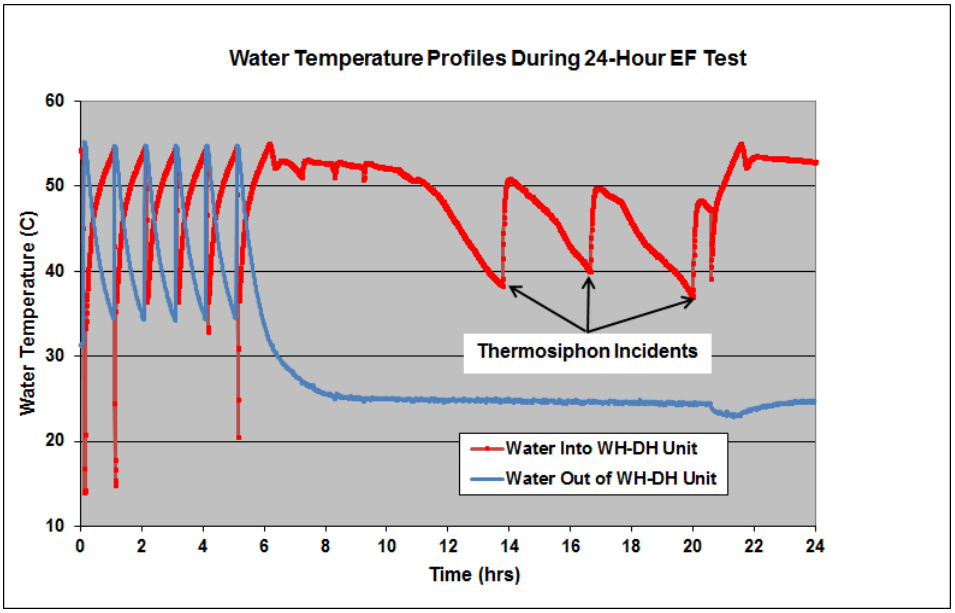

Figure 10. WH/DH EF test water inlet and outlet temperatures (Rice et al. 2014).

The final WH COP values versus EWT are shown in Figure 11 for the three indoor conditions. While the WH EF performance was increased substantially from the initial tests, the unit was still losing up to 23% of the available WH energy at 130 °F (54.4 °C) EWT. It is expected that insulation applied at the factory could reduce this loss by about half and enable achieving the EF target of ≥2.0.

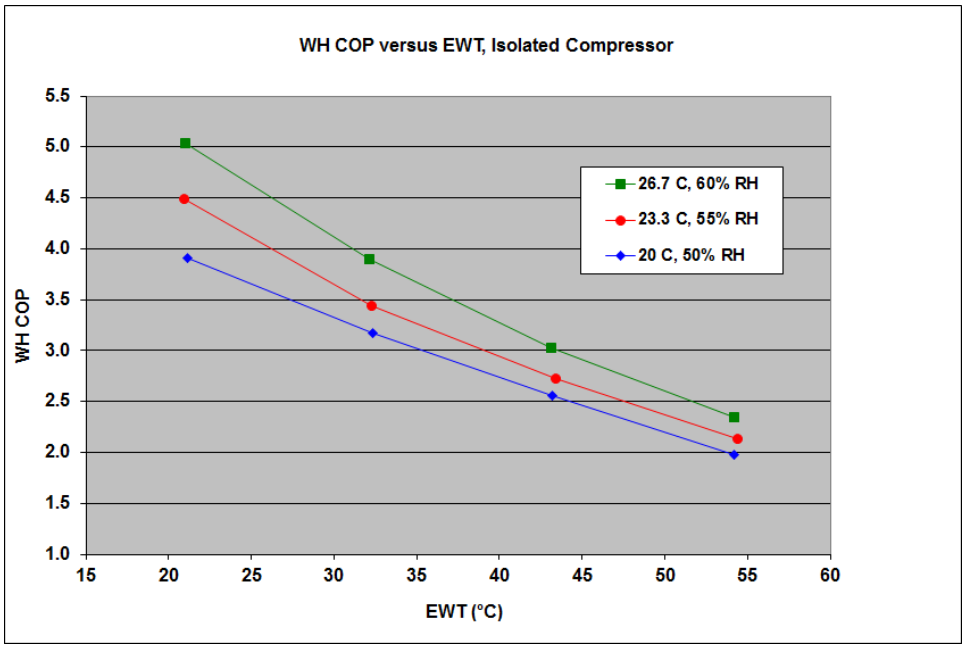

Figure 11. Final steady-state WH COP test results—Prototype 1 (Rice et al. 2014).

4. ANNUAL ENERGY USE ANALYSIS AND SAVINGS PREDICTIONS FOR AS-IHP BASED ON FIRST WH/DH PROTOTYPE DESIGN

The steady-state DH and WH data were used to recalibrate the HPDM for use in generating WH/DH unit performance maps for each mode. These maps were input to a customized project in the TRNSYS annual simulation model to estimate the expected energy savings for the AS-IHP prototype design. For preliminary estimates (Table 6), the same two-speed ASHP and an assumed 64.3 gal/d (243 L/d) hot water load (see Figure 12) were used. The TRNSYS simulations used a 3-min time step. Simulations were run for three DOE/BTO Building America climate regions (U.S. DOE 2013)—mixed–humid (Atlanta), hot–humid (Houston), and cold (Chicago)—in a 2600 ft^2 (242 m^2) tight, well-insulated two-story (i.e., nZEH) house. The same minimum efficiency all-electric baseline system was used for the updated analyses. For the baseline system, ventilation air was drawn into the envelope from continuous operation of bathroom exhaust fans while for the AS-IHP this air was supplied on the return side of the duct system as shown in Figure 3.

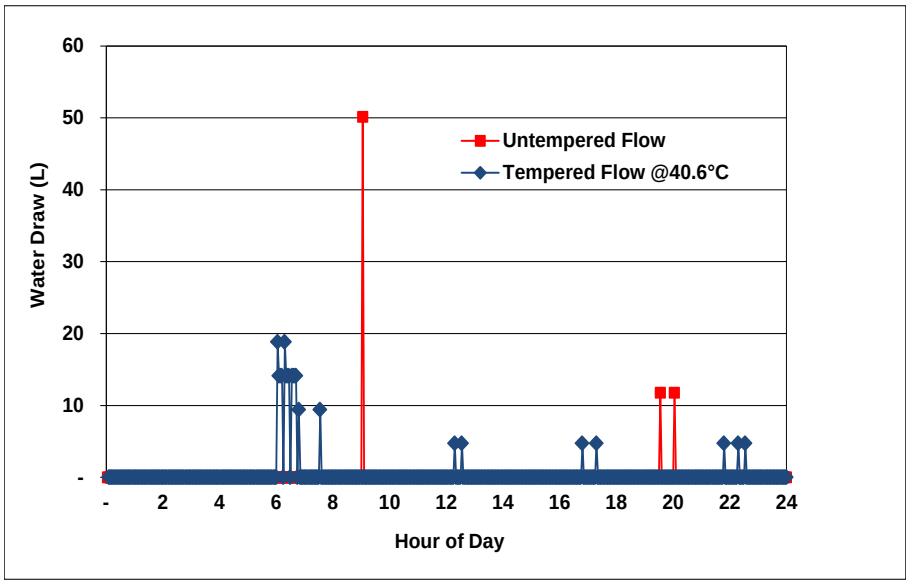

Figure 12. Assumed daily hot water draw schedule from DHW tank (Rice et al. 2014).

The preliminary simulations (Table 6) were performed at the optimal 300 cfm (142 L/s) for the WH/DH unit with operation allowed at all indoor blower speeds. However, blower test results for the prototype WH/DH module indicated that it could achieve only 240 cfm (113 L/s) airflow when the ASHP blower was operating at low speed. At high speed, the static pressure head on the WH/DH unit would be too high to achieve acceptable airflow. Accordingly, the revised TRNSYS simulations reported in Table 8 below were made with performance maps for 240 cfm airflow, and WH/DH operation was not allowed in conjunction with high-speed central heat pump operation. The average reductions in WH capacity and COP at the lower airflow rate were 3.2% and 3.4%, respectively, compared with the same values for 300 cfm airflow. The DH EF and water removal values at the rating point dropped 1.2% and 6.5%, respectively.

Comparisons of predicted energy use and savings between the baseline suite and the reduced flow case are shown in Table 8 for each mode and overall. The total predicted HVAC/WH energy savings for the reduced airflow and operation assumptions range from 33 to 36%, reduced slightly from the preliminary analyses shown in Table 6. The entries in red show the portion of the total energy use for each mode due

to resistance heat. The net space conditioning savings for the three cases for the AS-IHP combination range from 23% for Chicago to 25% for Houston. SH savings are reduced by the cooling effect of the WH/DH unit when in WH mode in the winter months, while the SC energy savings are enhanced. Predicted WH-only energy savings ranged from 50% in Chicago to 59% in Houston for the nominal WH set point of 120 °F (48.9 °C).

The annual electrical energy that is required to provide space conditioning, active DH, WH, and ventilation for these energy-efficient homes is modest. The web-based program, PVWatts (Dobos 2013) can be used to size a solar photovoltaic (PV) array to provide a specified energy requirement at a particular geographic location. A commercially available ASHP (Lennox 2013a, 2013b), compatible with this system, can accept solar PV as a second power source. The team investigated how many 275 dc watt solar modules would be needed to offset this annual electrical energy requirement for each city. For Atlanta and Houston, thirteen modules and fifteen modules, respectively, should be adequate to supply the annual electric power needs of the AS-IHP system. For Chicago, the maximum of sixteen solar modules would still leave a shortfall of 2157 kWh.

Table 8. Energy use and savings predictions for AS-IHP with reduced flow WH/DH unit configuration (Rice et al. 2014)

Energy Use by Mode; 242 m^2 Tight, Well-Insulated House			
	1-Speed Base	2-Speed w WH-DH Unit, 113 L/s	
Operation Mode	Energy Use kWh (I^2R)	Energy Use kWh (I^2R)	Reduction from Base (%)
Atlanta			
space heating	2311	1965	15.0%
resistance heat	(18)	(31)	
space cooling	1741	1059	39.2%
water heating	3380	1553	54.1%
resistance heat	(3380)	(488)	
dedicated DH	319	299	6.2%
ventilation fan	189	202	-6.9%
totals	7941	5079	36.0%
Houston			
space heating	995	906	9.0%
resistance heat	(0)	(3)	
space cooling	3035	1975	34.9%
water heating	2813	1169	58.5%
resistance heat	(2813)	(246)	
dedicated DH	1154	1035	10.3%
ventilation fan	189	179	5.6%
totals	8187	5264	35.7%
Chicago			
space heating	6214	4915	20.9%
resistance heat	(916)	(669)	
space cooling	740	402	45.6%
water heating	4218	2122	49.7%
resistance heat	(4218)	(906)	
dedicated DH	154	154	0.0%
ventilation fan	189	169	10.5%
totals	11514	7762	32.6%

Table 9 compares the WH load fraction for the larger home used in the analyses reported in Tables 6 and 8 (2.2-ton SC design load and capacity) with that for the smaller nZEH-ready house used in the concept analyses (1–1.5-ton SC design load/capacity). The WH load fractions for the larger house are slightly lower than those for the smaller concept house.

Table 9. WH load fraction for 2600 ft^2 house used in Table 6 and nZEH-ready house (Table 2)

Location	WH load fraction (% of total SC+SH+WH load)	
	Table 6 house	Table 2 house
Atlanta	20	22
Houston	16	18
Chicago	19	21

5. SECOND-GENERATION WH/DH PROTOTYPE AND AS-IHP FIELD-TEST SYSTEM DEVELOPMENT

WH/DH second-generation prototype development and lab test results

A second-generation WH/DH prototype was built and tested by Lennox in 2014. It used the same compressor and DH mode condenser as the first unit. A brazed-plate W/R HX replaced the tube-in-tube design to provide a lighter-weight, more compact, and easily insulated design. New, thicker 3/8 in. (9.5 mm) closed-cell neoprene sheet was used to insulate the W/R HX, and it was located in a position less exposed to the air stream. The tube-in-tube W/R HX of the first prototype was insulated with 1/8 in. (3.2 mm) neoprene tape. This together with its size and location led to the high heat losses noted above.

In addition, larger air duct inlet and outlet duct collars were implemented to reduce the static pressure drop in the unit and improve airflow capability. The evaporator refrigerant circuiting was also modified to increase the surface utilization. A photo of the second-generation prototype is provided in Figure 13; note the more open design relative to the first prototype (Figure 8) and the insulated brazed plate WH condenser.

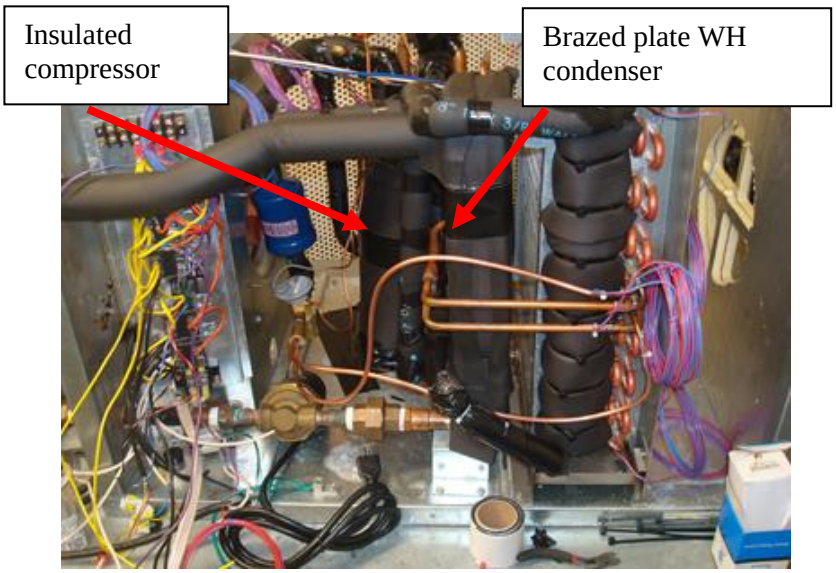

Figure 13. Second-generation WH/DH module prototype.

As noted above, the new module has larger-diameter duct collars (10 in. vs. 8 in. [254 mm vs. 203 mm]) in the first design) to reduce the static pressure drop unit and improve its airflow capability. Blower tests were run over a range of external static pressure (ESP) conditions, and Figure 14 illustrates the improvement compared with the previous design—about a 75% increase in ESP head capability at the design flow rate of 300 cfm (142 L/s). This improved blower capability should enable the second-generation WH/DH to reach the design airflow when connected to a central duct system, which should boost WH capacity and COP by about 3.3%. As noted earlier, the initial WH/DH prototype was limited to about 113 L/s (240 cfm). With higher cfm and static head, the second-generation design should also be able to operate with the ASHP blower at its top speed if the central duct system has a max ESP of 0.35 in. wg), whereas the previous unit could operate only when the heat pump was at low-stage capacity.

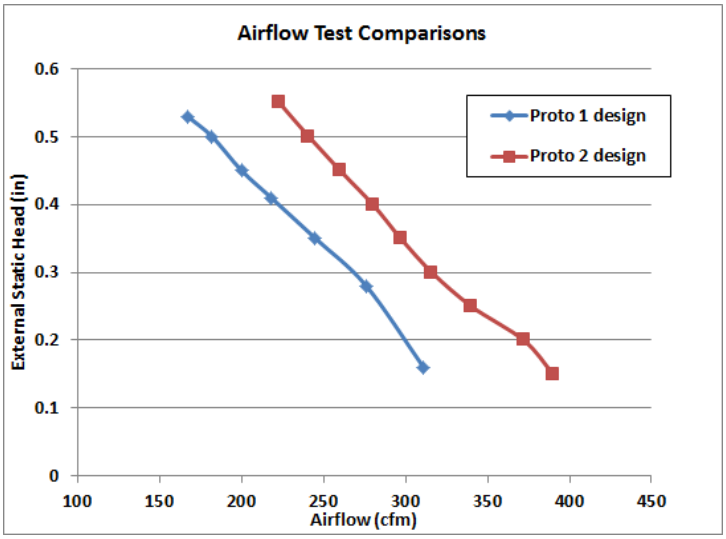

Figure 14. Second-generation prototype blower performance vs. first-generation blower.

Results from the initial WH mode 24-h use tests approximating the DOE EF test for HPWHs show reasonably good performance, given that it was likely undercharged, but the results strongly suggest that the thermosiphon effects that plagued the earlier tests of the first-generation unit also occurred in these tests. This caused an additional heat upcycle near the end of the 24-h test that penalized performance. Risers were added to the connecting lines between the DHW tank and the WH/DH unit and were found to reduce the thermosiphon effects considerably. In addition, the tank-to-WH/DH water line connection approach was revised from the original (where water was drawn from the dip tube and returned to the bottom of the tank) to use of a coaxial fitting at the bottom of the tank (Figure 15). Finally, the refrigerant charge was increased to raise the subcooling levels closer to design conditions.

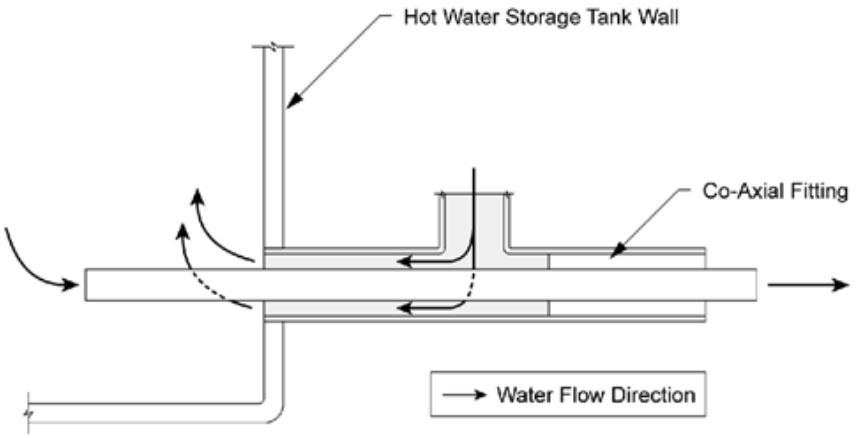

Figure 15. Schematic of coaxial tank water fitting.

After these modifications were completed, new ratings tests approximating the DH and WH EF conditions (within the limitations of the test facility capabilities) were run at Lennox. DH mode tests of the second-generation prototype have shown about a 7% improved DH EF relative to that for the first prototype: ~2.2 L/kWh vs. ~2 L/kWh for prototype 1 (exceeding the current Energy Star requirement (Energy Star 2016)). This appears to be due to the improved evaporator refrigerant flow distribution and more uniform airflow over the evaporator and condenser from the larger inlet/outlet ducts. WH mode test results showed an EF of ~2.05, slightly exceeding the WH performance goal for the project. Lennox also reported that the new coaxial water line connection maintained better tank stratification than with the original arrangement.

WH/DH and AS-IHP system field test prototype design

After completing lab tests of the second-generation WH/DH, Lennox modified the design to create a field-test prototype. The field-test design is generally based on the prototype 2 architecture implementing its operating mode efficiency improvements. A revised, solid-state control system was specified based on a UNO model solid-state microcontroller manufactured by Arduino, eliminating many of the relays used in the second-generation lab prototype. Figure 16 presents a photo of the field-test WH/DH unit with side panels removed to show the control board. Figure 17 provides a CAD drawing of the general layout of the field-test prototype WH/DH design. A list of its component parts is given in Table 10.

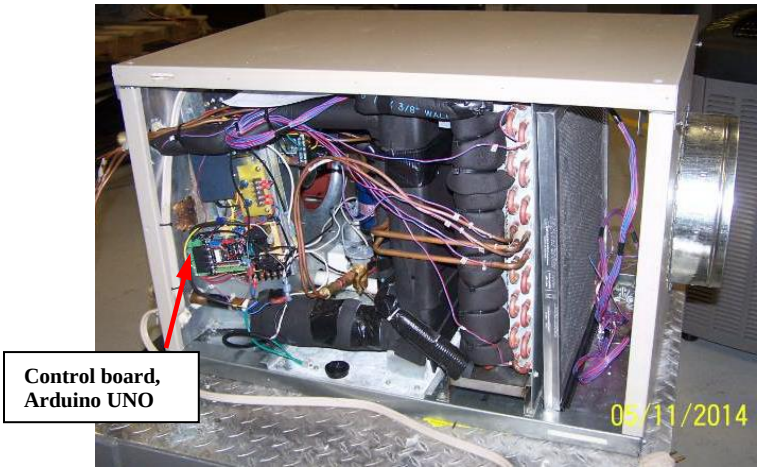

Figure 16. Field-test WH/DH prototype.

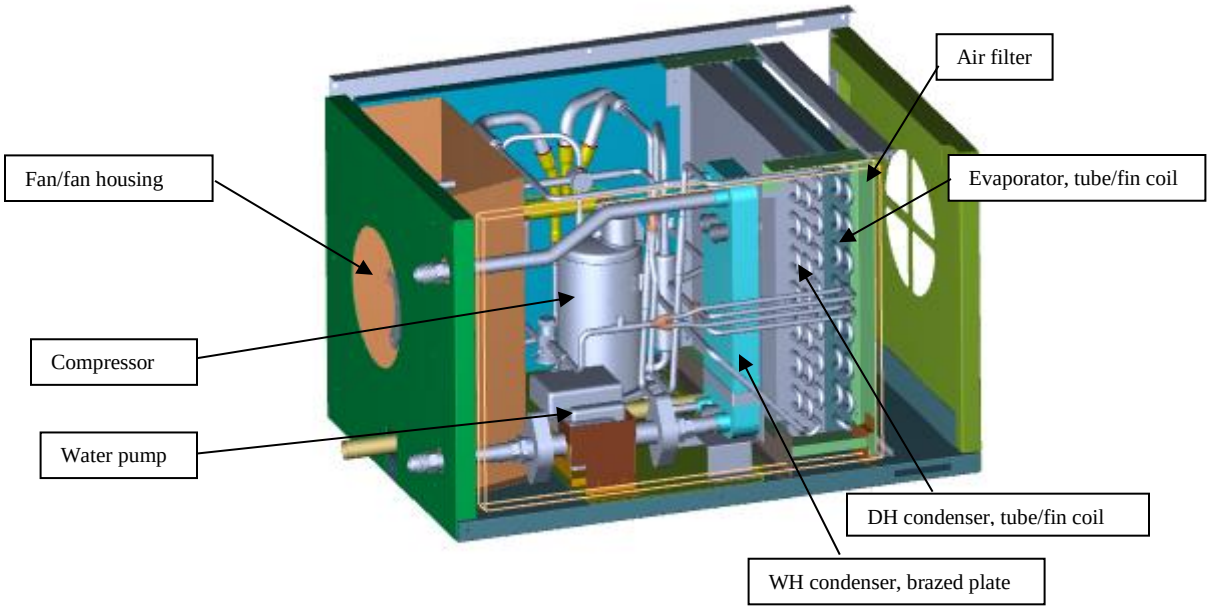

Figure 17. CAD drawing of field-test prototype WH/DH module.

An artist's representation of the AS-IHP field-test system arrangement is provided in Figure 18. The system design intent was to pair the WH/DH field-test prototype with a Lennox high-efficiency, VS XP-25 ASHP. The XP-25 family of ASHP products has rated SEERs of 20–24 and HSPFs of 9.5–10.2 (Lennox 2014) compared with the SEER of 18.4 and HSPF of 9.1 HSPF of the XP-19 unit used for the annual performance analyses reported in Tables 6 and 8. The model selected for our field-test AS-IHP was rated at 34.4 kBtu/h (10.1 kW) of cooling, with a SEER of 21.5 ($SCOP_c$ of 6.3) and DOE Climate Region IV HSPF of 10.0 ($SCOP_h$ of 2.9) (Air-Conditioning, Heating, and Refrigeration Institute [AHRI] 2016). Major components of the WH/DH are a single-speed (SS) compressor, SS water pump, VS fan, fin-and-tube refrigerant-to-air evaporator, brazed plate refrigerant-to-water condenser, and fin-and-tube refrigerant-to-air condenser, as depicted in Figure 17, above. A solid-state microcontroller manages competing requests for service, with WH having priority over DH. The VS blower initially used the same speed for WH, DH, and fresh-air V modes. Early in Summer 2016, a control change was implemented to slow down the WH/DH fan during V mode (see details in the DH performance discussion below).

Table 10. Field-test WH/DH prototype unit key components list

DESCRIPTION	Supplier	Part #	Qty
DISTRIBUTOR	SPORLAN	D260-2-3/16-1/6	1
VALVE-REVERSING + COIL (mode selection)	SAGINOMIA	STF-C13U6G3 + STF 615W	1
VALVE-EXPANSION	SPORLAN	BBIZE-1/2-GA-B10	1
ASSY-BRAZED PLATE HEAT EXCHANGER	SWEP	B16DWx12H/1P	1
VALVE-CHECK, 3/8 in.	WATSCO	3/8 in. MAGNACHECK	2
COMPRESSOR, 115 VAC	TECUMSEH	RG103AR-501-A41V	1
CONTROLLER, BLOWER SPEED	(LENNOX)	VSPC-4	1
ASSY-COIL, CONDENSER	(LENNOX)	JSJ-313-COIL	1
ASSY-COIL, EVAPORATOR	(LENNOX)	JSJ-313-COIL2	1
PUMP	LAING THERMOTECH	E3-BCSVNN3W-11	1
CONTROLLER, MICRO	ARDUINO	UNO	1

PAN-DRAIN, (ASSEMBLY)	(LENNOX)	JSJ-322-XX	1
RELAY	(LENNOX)	69J5601	3
TRANSFORMER	(LENNOX)	TBD	1
ASSY-BLOWER	EBM	R3G220AD	1
RING, VENTURI	EBM	TBD	1
AIR FILTER	(LENNOX)	TBD	1
TERMINAL-STRIP, 5 POSITION, 24VAC	(LENNOX)	TBD	1

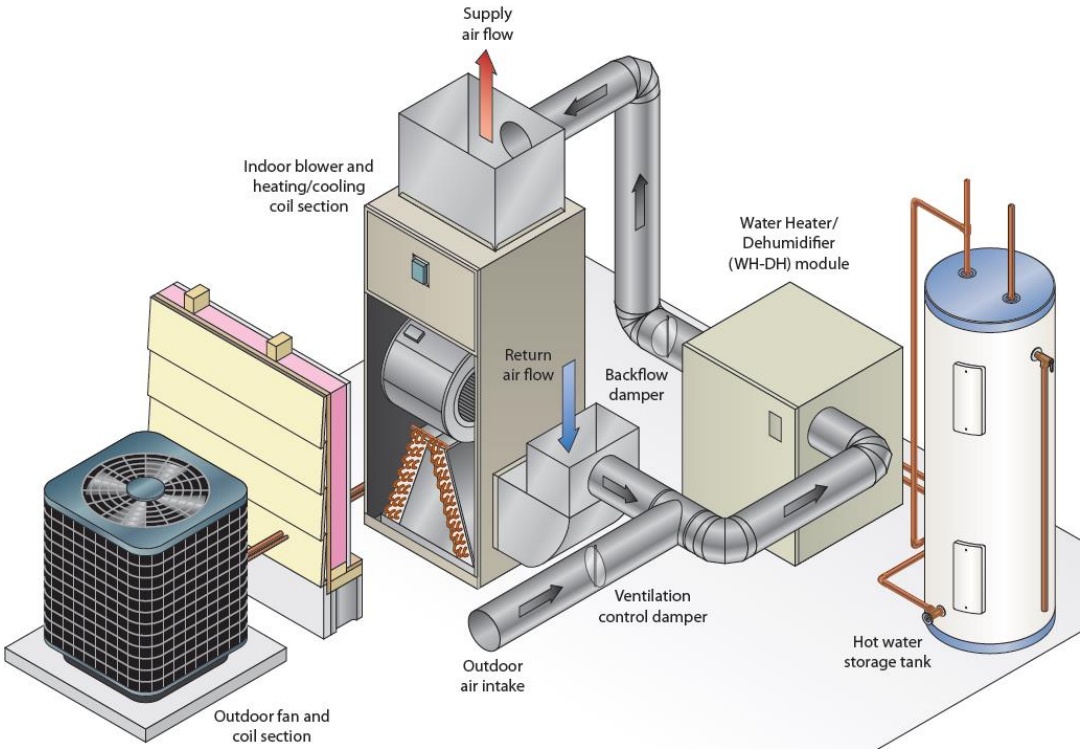

Figure 18. Two-unit AS-IHP field-test system arrangment.

6. FIELD-TEST SYSTEM PERFORMANCE AND ANALYSIS

The XP-25 ASHP and WH/DH prototype were shipped to ORNL in early 2015 and installed in June/July 2015 at a 2400-ft^2 test house (Figure 19) in Yarnell Station subdivision, in Knoxville, Tennessee, to facilitate a one-year field test. A photo of the field-test system is included in Figure 20 with the field data acquisition system (DAS) shown in Figure 21. Dutch Uselton of Lennox visited the test site on July 7-8, 2015, for startup of the WH/DH module and system commissioning. Full data monitoring of the AS-IHP system began in August 2015 and continued through September 2016. Monitoring of the WH/DH module continued through May 2017 to evaluate the impact of some design and control modifications implemented because of the initial test-year results.

Figure 19. Field-test site.

Figure 20. Field-test prototype in installation process. ASHP indoor air handler and WH/DH prototype shown with rain gauges for condensate collection (to monitor DH and latent cooling loads).

Figure 21. Field data acquisition system.

Before the field testing started, work was done to set up the test house occupancy simulation. The water draw schedule used at the site is based on the latest Building America water draw generator (DOE/BTO Building America Program, 2013). Latent, sensible, and other building internal loads are based on the Building America House Simulation Protocols (Hendron and Engebrecht 2010). Occupancy simulation devices follow a schedule that is input via a database that is read by a programmed controller for operating space heaters to simulate sensible heat, and humidifiers to simulate latent heat. Hot water loads (e.g., dishwasher, clothes washer, showers, sinks) are simulated by operating solenoid- controlled water valves according to the programmed schedule, with an average hot water use of 56.3 gal/day. Figure 22 shows the hot water valves and controller setup.

The DAS was set up to collect data at 15 s intervals with 1 min, 15 min, 1 h, and daily averages. Data were stored on servers located at ORNL. A dedicated internet connection was set up that allowed the Lennox project team to monitor data collection in real time.

Figure 22. Hot water use control valves.

WH/DH and AS-IHP system field-test prototype design

Equipment setup. The space conditioning system included zone controls and dampers that allowed the upstairs and downstairs zone temperatures to be controlled independently. The zoning system also controlled the ASHP airflow based on fixed airflow values that were assigned to each zone during commissioning of the system. The thermostat set points were 71.0 °F (21.7 °C) and 76.0 °F (24.4 °C) for the heating and cooling seasons, respectively. The ASHP operating mode was switched manually between heating only and cooling only as needed.

The WH/DH was connected to a standard electric storage water heater with copper pipe and a concentric fitting that was inserted in place of the typical drain at the bottom of the water heater. The power to the lower thermostat/element was disconnected and rewired to provide a low-voltage signal to the WH/DH when WH was required.

The return air for the WH/DH was ducted from the return plenum of the heat pump. The supply air was ducted separately from the WH/DH, with one duct terminating on the upstairs level of the house and the other terminating on the lower level. The WH/DH supply air can also be ducted into the supply air plenum of the heat pump if the supply fan of the heat pump is wired to operate at the same time as the WH/DH fan to prevent recirculation. Controlled fresh-air intake is one difference between the field-test system and the baseline equipment. A constant 45 cfm (21 L/s) of outdoor air was provided to the house. Homes with tightly sealed envelopes need mechanical fresh-air ventilation to maintain acceptable indoor air quality.

Instrumentation. The ASHP was instrumented for air-side heating and cooling capacity measurements as well as additional measurements of refrigerant-side pressures and temperatures. The condensate drained from the evaporator coil was also measured to provide a check on the air-side latent capacity

measurement. The WH/DH was instrumented for water-side WH capacity measurements as well as air-side capacity measurements for DH and the cooling byproduct from the WH mode. Like the ASHP, the condensate drained from the WH/DH was also measured to provide a check on the air-side latent capacity. Solid-state W/W transducers were used to measure the total and component energy use of the ASHP and WH/DH.

WH/DH dehumidification performance

During AS-IHP system test year (October 2015–September 2016). The WH/DH is called to dehumidify when a low-voltage alternating current (AC) signal is supplied. In a typical installation, this would be provided by a humidistat. However, since the home was already instrumented with humidity sensors, the data logger was used to provide the contact closure functionality of a humidistat. The call for DH mode was supplied to the WH/DH when either the Level 1 or Level 2 humidity sensors read over 55% RH, and was removed when both sensors read below 51% RH. The WH/DH did an excellent job of maintaining the humidity in the house, with the highest hourly average humidity measurement during the study being 54.8%.

One issue observed during WH/DH operation involved evaporation of condensate remaining on the evaporator coil during V mode (i.e., essentially all the hours when neither DH nor WH mode operation occurred). Both the DH and WH modes condense moisture from the air on the evaporator coil. This phenomenon can be seen in the top plot of Figure 23. The blue-highlighted sections indicate the unit operating in DH mode. In this mode, the unit is providing positive latent cooling and negative sensible cooling (i.e., heating). The house humidity is reduced as moisture is removed from the air. The pink-highlighted sections indicate operation in the V mode. In this mode, the unit is providing negative latent cooling (i.e., evaporating moisture into the air) and sensible cooling due to the evaporative cooling effect. This causes an increase in the house humidity and negates part of the work done during the DH mode. Based on a comparison of the air-side latent capacity during the DH mode and the latent capacity calculated based on the measured condensate leaving the unit, approximately 33% of the condensed moisture was being evaporated during the V mode. This results in an effective DH efficiency that is one-third lower than its steady-state efficiency. The first step taken to mitigate this effect involved reducing the airflow through the unit during the V mode. The initial equipment setup required the V airflow to be similar to that of the WH and DH (~300 cfm) to ensure the proper outdoor air V rate of 45 cfm. This was due to the small size of the fresh-air intake duct relative to the return duct of the WH/DH. In June 2016, a damper was added to the return duct of the WH/DH upstream of the fresh-air intake. This damper was closed during the V mode allowing the airflow to be reduced to the required V rate since the unit was now pulling 100% fresh air instead of a mixture of fresh air and house air. This action also significantly reduced the V mode fan power to ~13 W vs. ~53 W before installing the damper. The bottom plot in Figure 23 shows DH and V cycles of the WH/DH after the damper was installed, as well as reduced airflow composed of 100% fresh air for ventilation. During the V mode, the evaporation of condensate was significantly reduced, as indicated by the latent capacity being only slightly negative. The frequency of DH cycles was also reduced, and the humidity in the home increased at a much slower rate, although the outdoor conditions were slightly drier for the data shown in the bottom plot of Figure 23. Once again, a comparison between the air-side latent capacity measured during the DH mode and the condensate collected from the WH/DH indicated that only 5% of the condensed moisture was evaporated back into the air during the V mode. This is a significant reduction when compared with the 33% evaporation rate seen prior to the installation of the return air damper.

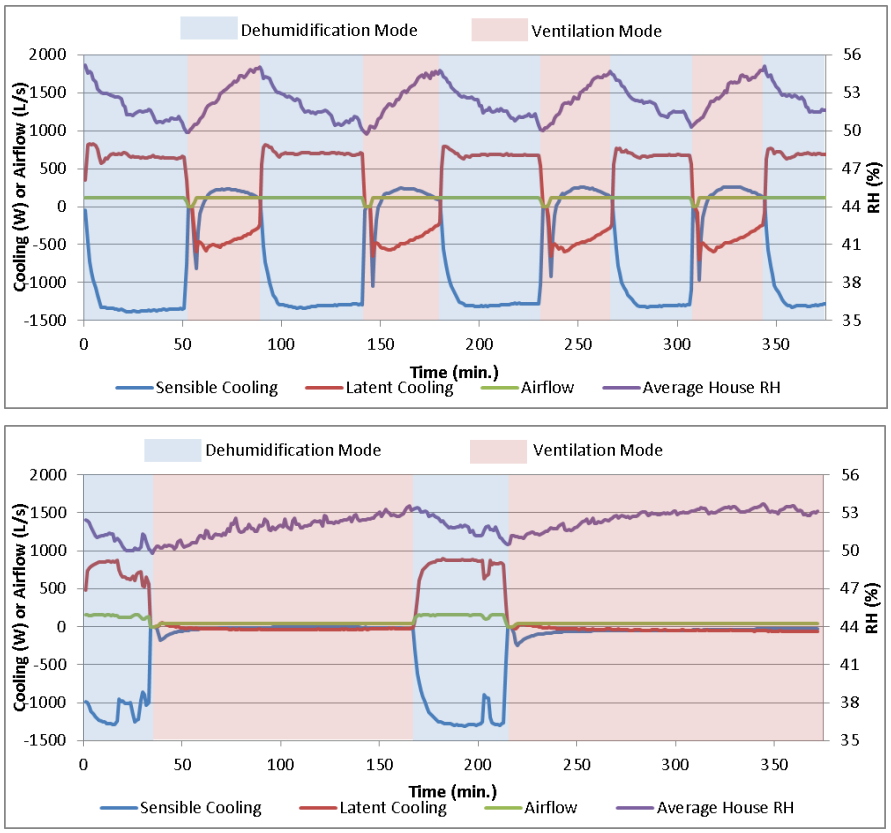

Figure 23. WH/DH cycling between DH mode and V mode with condensate evaporation during ventilation, for equal V and DH airflow rates (top plot) and with reduced airflow during V mode (bottom plot) (Munk et al. 2017).

The monthly runtime and average efficiency based on the measured air-side latent capacity are shown in Figure 24. As noted earlier, evaporation of condensate in the V mode likely resulted in increased DH runtime for all months prior to and including June 2016. July and August 2016 showed significant (i.e., >100 h per month) DH runtime due to high outdoor humidity. September 2016 had a higher average outdoor humidity than October to December 2015 but had significantly less DH runtime, illustrating the reduction in reevaporation of condensate during V mode. For the months with significant runtime, the efficiency for DH ranged from ~1.5-2.1 L/kWh. There were measurement issues related to the air-side capacity of the WH/DH for the months of August to October 2015, so this period was excluded from the calculation of the average DH efficiency of 1.7 L/kWh.

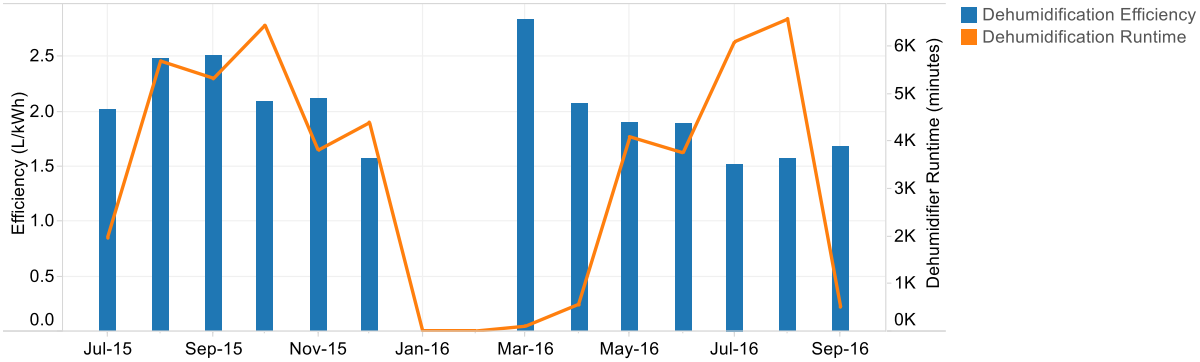

Figure 24. Monthly DH efficiency and runtime (Munk et al, 2017).

Further field tests to evaluate impact of WH/DH system and control design modifications. After the AS-IHP system field test was concluded, Lennox developed a design for an adjustable damper to block part of the WH/DH evaporator during the V mode operation. The intent was to further reduce the amount of condensate reevaporation during the V mode. This was implemented in late March 2017, and the modified WH/DH was tested with and without the damper for a few humid days in April 2017 to evaluate the impact of the design change. Test results showed no significant change in condensate reevaporation during V mode compared with reduced V mode airflow (Figure 23, bottom plot). While a significant portion of the evaporator was blocked by the damper, the exposed area had much- higher-velocity air travelling over it to maintain the same fresh-air ventilation rate. This higher velocity air results in locally increased evaporation rates and may explain why no significant change was seen in the overall condensate reevaporation rate. At this point the project had to be concluded to make way for other uses of the field-test site. The prototype WH/DH was shipped back to Lennox in May 2017.

WH/DH water heating performance

As noted earlier the hot water draw schedule varied from day to day based on realistic probability distributions of hot water draws. Figure 25 presents a histogram of the daily hot water use for the period of October 2015 to September 2016. The average daily hot water draw for this period was 55.2 gal/day (209 L/day), slightly below the target of 58.1 gal/day (220 L/day). This difference resulted from an issue with the hot water draw system that occurred in January 2016, resulting in 20 days of no hot water use.

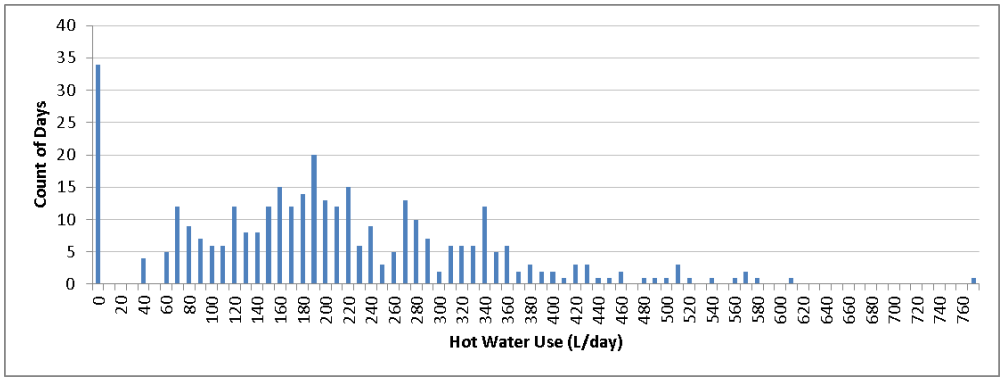

Figure 25. Histogram of daily hot water use at the research house (Munk et al. 2017).

The efficiency of a heat pump is impacted by the temperature of the heat source and the temperature of the heat sink. For the case of WH, the heat source is the air entering the WH/DH unit, and the heat sink is the entering water. Figure 26 shows a color map, based on 1 min resolution data, of the WH mode COP for various entering air and entering water temperatures experienced during field testing. As expected, the COP of the system increases with an increase in entering air temperature (i.e., heat source) and decreases with an increase in entering water temperature (i.e., heat sink), as seen by the color trend of red to blue from the lower right of the map to the upper left. The percentages located within each cell indicate the percentage of the total WH runtime at the given conditions. Most of the operating time occurs at higher entering water temperatures—95°F (35°C) and up—indicating that the bottom of the tank stayed relatively warm most of the time. During heavy hot water use, the lower portion of the tank can become saturated with cold water, resulting in entering water temperatures near the temperature of the cold water supply.

The WH/DH was set up to pull a mixture of house air and fresh air for V during WH operation. This approach maintains continuous V in the home and provides warmer, more humid return air during summer months. However, when it is cool or cold outside, the fresh air reduces the efficiency of the WH mode. During extremely cold weather, it is also possible for the evaporator to freeze. This occurred early

in the heating season and is represented by the low entering air temperatures and corresponding efficiencies (dark red) in Figure 26.. A control change was made during the heating season to close the fresh-air damper during WH operation when the outdoor temperature was below 60.0 °F (15.6 °C) to maintain higher WH efficiencies and eliminate the risk of the evaporator freezing.

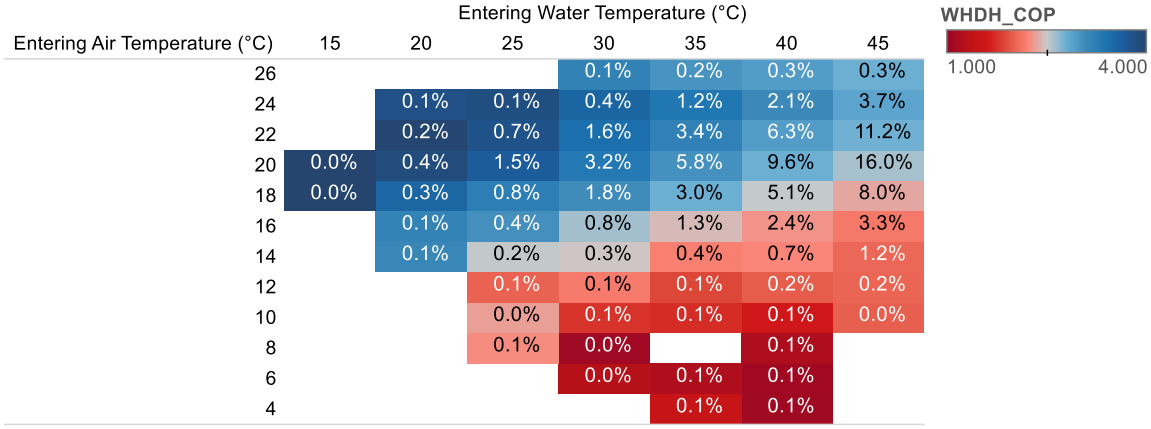

Figure 26. WH mode COP for various entering air and DHW temperatures with percentage of total WH operating hours labeled for each set of conditions (Munk et al. 2017).

The monthly WH efficiencies for the WH/DH are shown in Figure 27. The different lines indicate the performance of the system at various points as heat is generated by the WH/DH unit (heat pump), transferred to the storage tank, and then leaves the storage tank for use in the house. The blue line shows the COP of the heat pump only, which does not account for backup resistance heat use and losses associated with the interconnecting lines and storage tank. These COPs range from a low of 2.3 in January to a high of 3.1 in August. As mentioned earlier, there were no hot water draws for 20 days in January. Without the flow of cold makeup water into the tank, the entering water temperatures seen by the WH/DH will be at least as high as the lower thermostat “make” temperature of approximately 112 °F (44.4 °C). The higher entering water temperatures seen by the WH/DH when recovering from standby losses compared with recovering from hot water use resulted in lower than average COPs for the month of January.

The orange line in Figure 27 shows the COP of the WH/DH when accounting for heat loss in the water lines that connect the WH/DH to the storage tank. Immersion temperature sensors located on both ends of the interconnecting water lines allowed for the measurement of the heat loss. Despite the water lines being insulated, the measured heat loss from these lines averaged 9.8% of the heat provided by the WH/DH heat pump. Examining a one-week snapshot of data indicated that, on average, the water lines lost 76% of their heat relative to the garage temperature between WH cycles. With a total length of 35.8 ft. (10.9 m) of 0.75 in. (1.9 cm) diameter copper pipe and 2007 WH cycles, the heat loss between cycles of the water in the pipes and the pipes themselves is estimated to be 738 kBtu (216 kWh) or 6.2% of the WH delivered by the WH/DH. Using the average garage temperature, average water temperature in the lines, and insulation thickness, the heat loss from the lines during the WH cycle was calculated to be 453 kBtu (133 kWh) or 3.8% of the water heat provided by the WH/DH. Combining the calculated off-cycle and WH cycle line losses yields a calculated value of 10.0% heat loss, which agrees well with the measured line losses of 9.8%.

The green line in Figure 27 shows the COP of the system when including backup resistance heat use but excluding tank losses. After filtering the data for periods when the WH/DH was shut down for sensor maintenance or other issues, the backup resistance energy use for the yearlong period was just 60.2 kWh or 5.4% of the total energy used for WH.

Finally, the red line in Figure 27 shows the COP of the entire system. It was calculated by dividing the measured WH energy being delivered to the house at the outlet of the storage tank by the total energy use of the WH/DH and backup resistance elements. Based on the measured data, the tank losses are 9.9% of the WH energy delivered to the tank (omitting data from 20 January days of no hot water use). This value is in line with the performance expectations of a typical electric storage water heater tank having a rated EF of 0.9, the minimum allowable EF for electric storage WHs manufactured before April 2015 in the United States.

The annual WH mode COPs for the WH/DH were 2.75, 2.48, 2.39, and 2.19 for the heat pump only, heat pump with line losses, heat pump with line losses and backup resistance use, and entire WH/DH system including tank/line losses and backup resistance heat use, respectively. To achieve the highest overall system WH efficiencies, it is important to limit the length and diameter of the water lines connecting the WH/DH to the storage tank as much as possible, insulate these lines, and use a well-insulated storage tank.

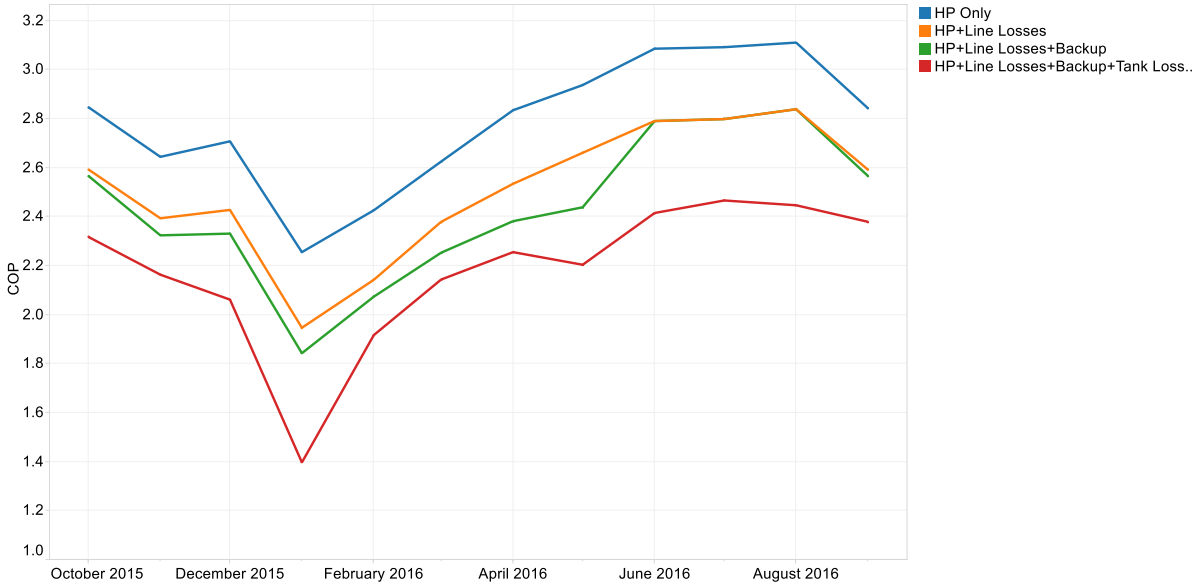

Figure 27. Monthly average WH mode COPs of the WH/DH heat pump with and without backup resistance heat use and heat losses from the storage tank and water lines connecting the WH/DH to the storage tank (Munk et al. 2017). *Note:* HP – heat pump.

AS-IHP space cooling performance

The monthly and seasonal SC performance of the ASHP and the impact of the WH/DH operation on SC are summarized in Table 11. The average monthly cooling COPs of the ASHP were between 4.32 and 5.59 with a seasonal average of 4.44. The WH mode of the WH/DH provides SC as a byproduct of its operation. The DH mode also generates sensible heating in addition to latent cooling with a net space heating effect, indicated by negative values in the table. The "free cooling" effect that the WH operation has on the overall AS-IHP system (ASHP and WH/DH combined) SC efficiency results in monthly cooling COPs for the system between 4.46 and 10.84. The very high system COPs during April and October are indicative of a larger ratio of "free cooling" from the WH/DH to cooling supplied by the ASHP. However, it is likely that much of the SC delivered by the WH/DH in these months was not satisfying a real demand for SC and the house was, in fact, being overcooled. Because of this, the WH/DH cooling effect for these two months was not included in the seasonal average SC COP for the system. With this consideration, the seasonal average SC COP of the system was 4.72, 6.3% higher than

the COP of the ASHP alone. For the cooling season, this 6.3% increase in efficiency results in estimated SC energy savings due to operation of the WH/DH of 122 kWh.

Table 11. SC data for the ASHP and AS-IHP system including the cooling and heating byproducts of the WH/DH (Munk et al. 2017)

Month	April 2016	May 2016	June 2016	July 2016	Aug. 2016	Sept. 2016	Oct. 2016	Totals
System SC delivered, kWh	191	674	1819	2317	2304	1812	271	9189[a]
ASHP	122	526	1697	2242	2233	1680	141	8641
WH/DH Mode	-4[b]	-30	-23	-56	-50	-5	-23[b]	191
WH/DH WH Mode	73[b]	178	144	132	121	137	153[b]	938
ASHP SC energy use, kWh	22	99	385	517	517	383	25	1948
ASHP Avg. COP	5.57	5.34	4.41	4.34	4.32	4.39	5.59	4.44
System Avg. COP	8.68	6.84	4.72	4.48	4.46	4.77	10.84	4.72[a]
Avg. OD temp, °C	15.7	18.9	25.1	26.4	26.3	23.7	15.1	21.6
while ASHP cooling	25.0	25.3	28.1	28.4	28.0	26.9	23.4	27.6
ASHP Run hours	22.5	95.0	300.5	400.3	409.7	329.3	31.4	1588.7

[a] Total system SC delivered and average system COP do not include WH/DH cooling/heating effects for the months of April and October because the cooling demand was very low for these months; therefore, it is likely that the WH/DH operation did not significantly affect the cooling load experienced by the ASHP.
[b] Only includes days of the month when the ASHP was in the cooling mode.

AS-IHP space heating performance

The monthly and seasonal SH performance of the ASHP and the impact of the WH/DH operation on SH are summarized in Table 12. As noted earlier, when the WH/DH operates in WH mode, it provides SC as a byproduct. However, for the heating season, the latent cooling provides no energy benefit or penalty, so the data shows only the sensible cooling. Similarly, for the limited runtime in the DH mode, only the sensible heating is accounted for in the table. The monthly SH COPs for the ASHP only are between 2.00 and 3.43. The lowest COPs correspond to months with high backup resistance heat use. For the month of January 2016, backup resistance heat use accounted for approximately one-third of the total SH energy use. The average SH COP of the ASHP during the evaluation period was 2.38. When the cooling and heating byproducts of the WH and DH modes of the system are accounted for, the overall AS-IHP system SH COP is reduced to 2.23, a 6.3% reduction. For the heating season, this 6.3% reduction in overall efficiency results in an estimated SH penalty due to operation of the WH/DH of 330 kWh.

Table 12. SH data for the ASHP and AS-IHP system including the cooling and heating byproducts of the WH/DH (Munk et al. 2017)

Month	Oct. 2015	Nov. 2015	Dec. 2015	Jan. 2016	Feb. 2016	March 2016	April 2016	Totals
Total Sensible Heating delivered, kWh	172	1344	1687	4029	2723	1192	384	11,651[a]
ASHP	171	1431	1764	4158	2974	1408	505	12,411
WH/DH Mode	43[b]	77	77	0	0	1	1[b]	199
WH/DH WH Mode	-42[b]	-164	-154	-129	-251	-216	-122[b]	-1078
Space Heating energy use, kWh								
Total	50	502	677	2076	1289	478	153	5225
backup	0	0	120	684	299	32	1	1136
defrost	0	0	19	54	24	8	0	105
Avg. ASHP COP	3.43	2.85	2.61	2.00	2.31	2.94	3.29	2.38
Avg. System COP	3.44	2.68	2.49	1.94	2.11	2.49	2.51	2.23[a]
Avg. OD Temp, °C	15.1	11.5	10.6	1.5	5.4	12.5	15.7	10.3
While ASHP heating	10.2	5.9	5.3	0.2	2.1	5.8	7.6	3.3
Run hours	27.0	260.2	289.2	592.0	449.0	241.3	87.9	1946.6
Defrost hours	0.0	0.0	4.0	10.7	5.1	2.1	0.2	22.1

[a] Total system SH delivered and average system COP do not include WH/DH cooling/heating effects for the months of April and October because the heating demand was very low for these months; therefore, it is likely that the WH/DH operation did not significantly affect the heating load experienced by the ASHP.
[b] Only includes days of the month when the ASHP was in the heating mode.

Both the SC and SH average measured seasonal efficiencies (COP or EER in Btu/Wh) for the ASHP unit deviated significantly from AHRI 210/240 (AHRI 2008) rated values, as seen in Table 13. The AHRI estimates were computed using both the minimum and maximum house load line or design heating requirement (DHRmin and DHRmax) assumptions and for the actual measured test house load lines for the 2015–2016 field-test period (Figure 28). In Figure 29, these heating and cooling loads are shown compared with the AHRI 210/240 heating and cooling load lines based on the rated heating capacity Q(47) at 47 °F (8.3 °C) ambient and the rated cooling capacity Q(95) at 95 °F (35 °C).

Table 13. Site-measured seasonal SH and SC COPs vs. estimated AHRI 210/240 ratings for ASHP unit used in AS-IHP system

Mode	Site-measured COP (EER in Btu/Wh)	AHRI 210/240 ratings (Btu/Wh)	% deviation, field vs. rated
SH	2.38 (8.12)	Region IV HSPF:	
		For DHRmin load—10.00[a]	−18.8
		For DHRmax load—7.59	+7.0
		For house loads—7.98	+1.8
SC	4.44 (15.15)	SEER:	
		For default load and Cd—21.50[1]	−29.5
		For house loads—23.55	−35.7

[a]From AHRI (2016)

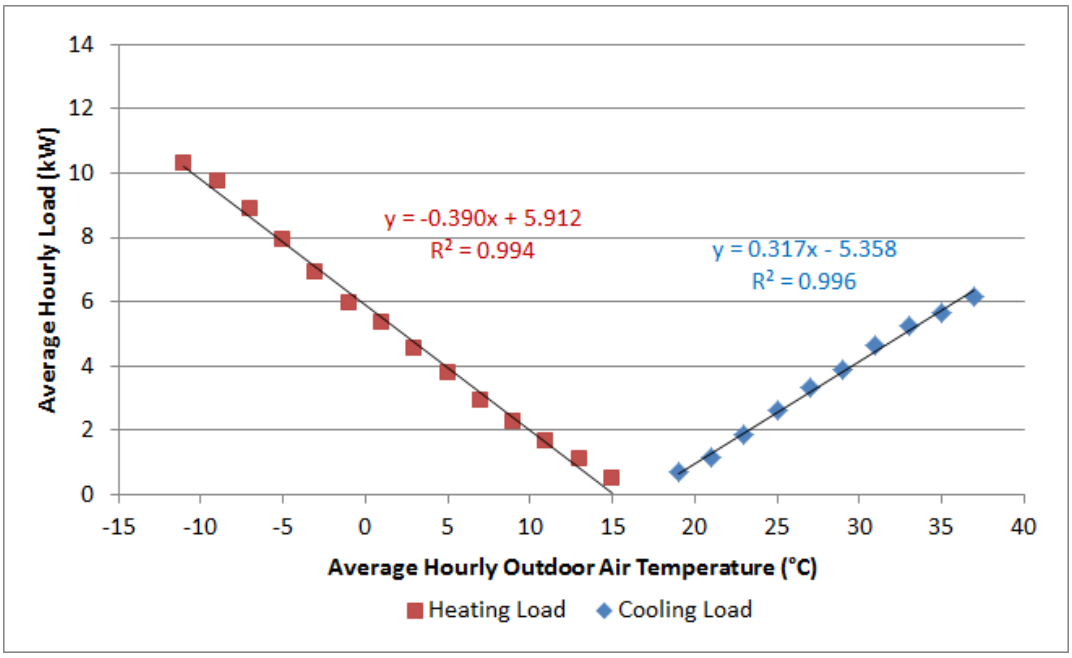

Figure 28. Field-test house 2015–2016 heating and cooling load lines

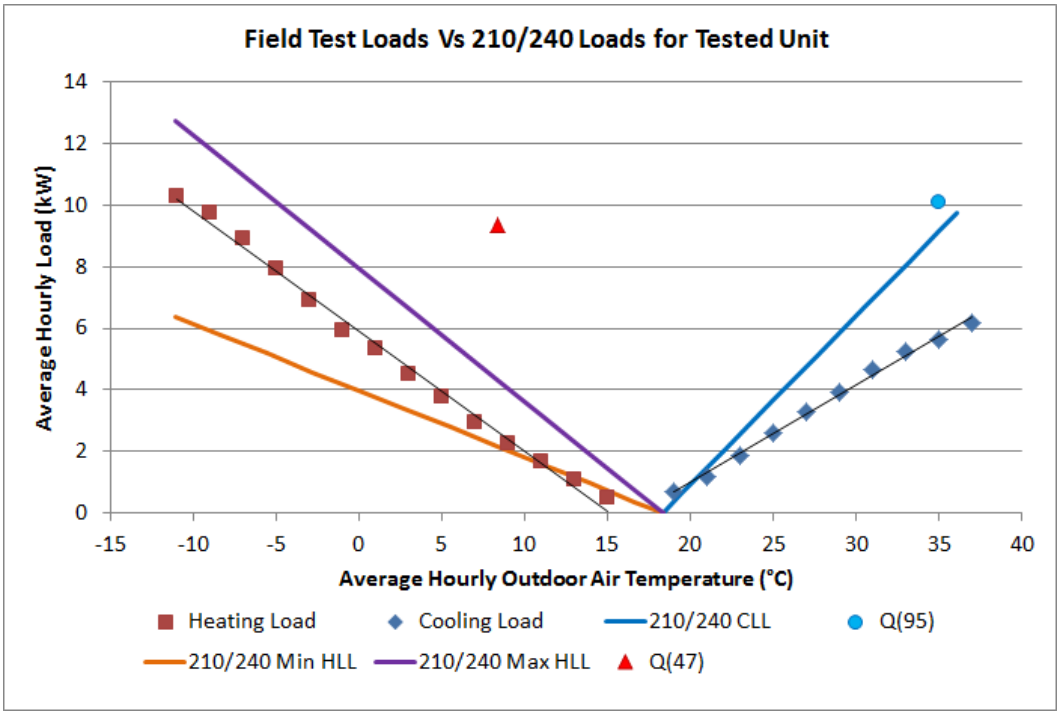

Figure 29. Field-test house 2015–2016 heating and cooling load lines vs. AHRI 210/240 load lines (max and min).

There are several reasons why the ASHP of the AS-IHP field prototype might show these deviations compared with its rating values:

- Blower energy use is higher at the field site due to higher duct system ESP losses than those assumed for the rating calculations. This is somewhat peculiar to the zoned distribution system used at the test

house and to other changes made in the ducting system to accommodate the AS-IHP. In general, however, residential duct systems have higher ESPs than that implicitly assumed in AHRI 210/240 (0.15 in. water gauge).

- The two-zone duct system in the test house caused the ASHP to operate at higher speeds than the space loads would warrant during times when both zones simultaneously called for SC or SH (Munk et al. 2017). This reduced the energy savings that could have accrued from lower speed operation during mild weather periods in both SH and SC seasons. (The effect was greater in the SC season.) Additionally, the data indicates that the compressor speed was allowed to vary even though the supply airflow was dictated by the zone(s) calling for conditioning. This results in the system running at suboptimal combinations of compressor speed and airflow, also reducing efficiency. See further discussion on this point in the next section.

- The HSPF procedure does not account for defrost tempering heat usage. This accounted for ~2% of the total field system SH energy use during the test year.

- The indoor temperature during the heating season averaged 71.4 °F while the HSPF calculation procedure assumes 70 °F.

- The indoor DB temperature during the cooling season averaged 76.0 °F while the SEER procedure assumes 80 °F. Additionally, the SEER procedure uses a 67 °F wet bulb temperature while the house condition was maintained at less than 64.5 °F wet bulb.

- The standard minimum house load line used in the HSPF procedure has a lower slope than that experienced at the test house this winter (see Figure 29). This results in a lower design heating load than that experienced by the test house. This is a primary reason that ~22% of the total SH seasonal energy use for the field-test system was from backup resistance heat (Table 13), even though the 2015–2016 SH heating season in Knoxville was warmer than average, having ~18% fewer heating degree-days based on the local airport weather station (Table 14). Note that in the TRNSYS simulations (Tables 6 and 8), resistance heating use was ~14% of the total in Chicago and <2% in Atlanta and Houston. With a significant amount of resistance heat usage (cf. the Chicago case in Tables 6 and 8), the potential annual energy savings for an AS-IHP drops significantly.

- The test year cooling season in Knoxville was significantly warmer than average, having ~39% more cooling degree days as measured at the local airport weather station (Table 14). This resulted in many more hours of high-speed operation during SC than normally expected, adding to the impacts from the zoned duct system noted above.

Table 14 compares average heating and cooling degree days for Knoxville to those experienced during the 2011–2012 and 2015–2016 test years. The table provides the average degree days for the three simulation locations as well for comparison.

Table 14. Average vs. 2015–2016 test site heating and cooling degree days

Location	Annual °F days heating (65 °F base)	Annual °F days cooling (65 °F base)
Atlanta[a]	2671	1893
Houston[a]	1371	3059
Chicago[a]		
O'Hare	6209	864
Midway	5872	1034
Knoxville		
Average[a]	3594	1514
2011–2012[b]	2796	1725
2015–2016[b]	2955	2106
2015–2016[c]	3301	1926

[a]1986–2010 averages from ASHRAE (2013).
[b]Test year actual values from National Oceanic and Atmospheric Administration (NOAA 2015, NOAA 2016) for McGhee Tyson Airport weather station.
[c]For test year October 2015–September 2016; site-measured actual.

Estimated AS-IHP annual energy savings based on field results

Bin-hour estimation analysis. For this savings estimation approach, the hourly SH loads and sensible and latent SC loads delivered by the AS-IHP were averaged within 3.6 °F (2.0 °C) outdoor air temperature bins. Note that the house load was calculated as the net delivered heating/cooling of the ASHP and WH/DH, which includes any conditioning needed to compensate for the ventilation load. This provides the average house heating and cooling loads as seen in Figure 30. As shown earlier, the heating load line for this house is about 50% higher at the DOE Region IV heating design temperature of 5 °F than the heating load line used for HSPF ratings calculations. The performance of the baseline equipment (ASHP with rated performance of 3.8 $SCOP_c$, 2.3 $SCOP_h$ (SEER of 13, HSPF of 7.8), and cooling capacity matching the AS-IHP system for space conditioning, a 0.9 EF water heater, and a 1.4 EF dehumidifier) was calculated using performance curves obtained from BEopt version 2.4.01 (NREL 2015 and underlying equations used in EnergyPlus (DOE 2016). The performance curves and equations accounted for increased field-installed fan power, frosting and defrosting effects, tempering heat during defrost cycles, cycling losses, and return-air conditions matching those of the AS-IHP system. It was assumed that excess latent capacity of the baseline system reduced the return-air humidity to the point that there was no longer any excess latent capacity. When additional latent capacity was required the dehumidifier and heat pump ran to provide the necessary latent capacity with a net sensible heating capacity of zero. The average power of the equipment required to meet house loads was calculated for each bin. The seasonal energy use and total delivered loads were calculated by multiplying the number of hours in each bin (Figure 31) by the corresponding power and required capacity. For this approach, the latent SC provided by the WH/DH during the heating season was ignored.

The results of the bin–hour analysis are shown in Table 15. The AS-IHP system shows significant savings in all modes of operation except for SH; comparatively lower savings for SH is due to the atypical heating load and zone control discussed below. The ASHP used in the field test achieves high efficiencies at part-load conditions but does not significantly "overspeed" the compressor at low temperatures to maintain heating capacity. This factor, in combination with the high backup electric SH energy use in January and February and SC penalty of the WH/DH operation in the WH mode, reduced the SH energy

savings. An annual savings of 28% (3270 kWh) was estimated for the AS-IHP system relative to the baseline equipment for the 2015–2016 test year.

While the zoned air distribution system ensured that both levels of the house were maintained at the desired conditions, the method of controlling the ASHP airflow based on the zone(s) calling for conditioning may have reduced the ASHP efficiency. Based on the data, it appears that the ASHP ran at a compressor speed corresponding to the airflow set for the zone(s) calling for space conditioning. For example, when both zones were calling for space conditioning, the ASHP ran at high airflow and correspondingly high compressor speeds regardless of the actual load on the house. Therefore, there were times when the ASHP ran at a higher capacity than necessary to meet the load on the house. This reduced the operating time of the ASHP at low capacity where it is most efficient and increased cycling and associated losses. Due to this, the SH and SC energy savings estimates are likely conservative, and additional savings could be expected of a system not operating with zone controls.

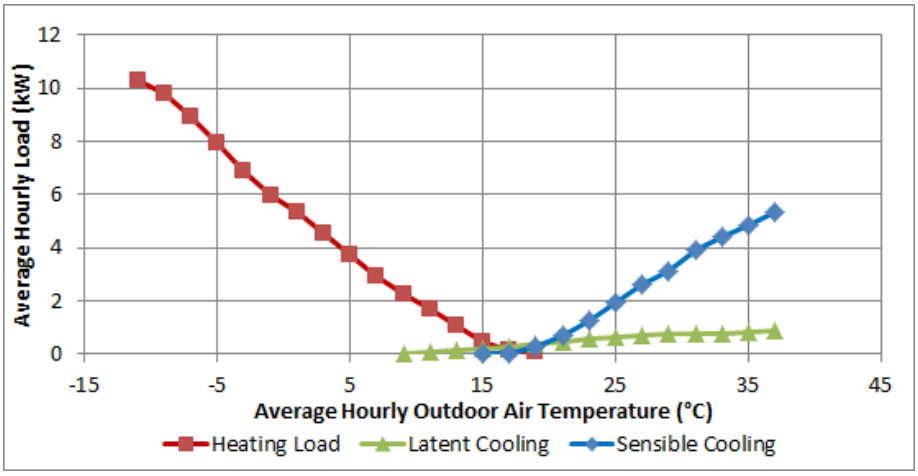

Figure 30. Average hourly heating, sensible cooling, and latent cooling loads of the field-test house (Munk et al. 2017).

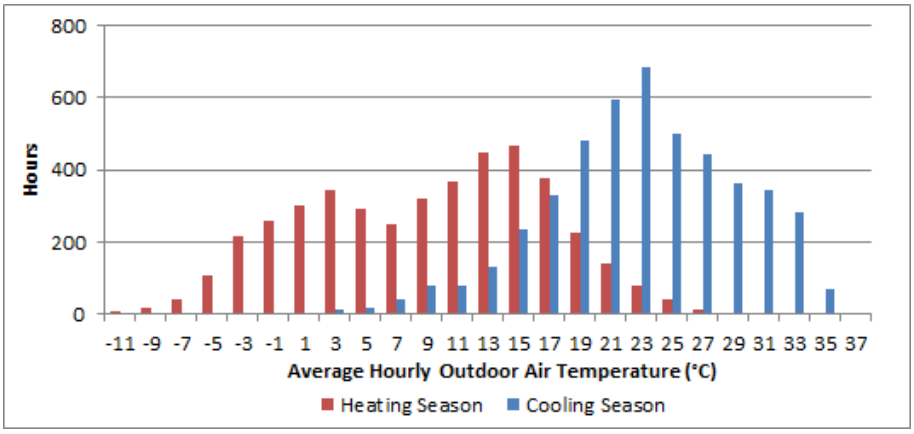

Figure 31. Cooling and heating season hours falling within outdoor air temperature bins (Munk et al. 2017).

Table 15. Estimated annual energy savings for the AS-IHP relative to baseline equipment – based on bin-hour analysis (Munk et al. 2017)

	Baseline	AS-IHP	Savings over baseline
Space heating (kWh)	5889	5225	11%
Space cooling and dehumidification (kWh)	3214	2201	32%
Water Heating (kWh)	2739	1146	58%
TOTAL (kWh)	11,842	8572	28%

Estimation based on prior baseline ASHP test results. Field measurements on two SS ASHPs were done in the Knoxville area in 2011–2012. Both were tested in a two-story house located within 5 miles of the Yarnell Station field-test house used for the AS-IHP field tests. SS unit 1 conditioned the downstairs, and unit 2 conditioned the upstairs. It should be noted here that the 2011–2012 actual weather was a bit warmer than normal: 22% warmer heating season and 14% warmer cooling season (Table 14). Heating season measurements showed field-measured COPs of 1.52 and 1.76 (EERs of 5.2 and 6.0) for units 1 and 2, respectively (Munk et al. 2013). These deviate from the AHRI 210/240 HSPF rating for the units of 7.7 (per AHRI 210/240 based on DHRmin load line) by -32% and -22%, respectively. In comparison, the measured seasonal SH efficiency of the VS ASHP of the AS-IHP system showed a -19% deviation compared with its HSPF- rating based on DHRmin load line (Table 13). For cooling operation, the two SS ASHPs had average measured seasonal COPs of 2.08 and 2.46 (EERs of 7.1 and 8.4), respectively, or -45% and -35% deviations from the rated SEER. The measured SC efficiency of the VS ASHP showed a -30% deviation from its rated SEER in comparison (Table 13).

Annual energy use of a baseline system (SEER of 13 and 7.7 HSPF of 7.7 for Region IV SS ASHP and electric WH) meeting the 2015–2016 field-test site loads was estimated as described below. Seasonal SH and SC efficiencies for the baseline unit were adjusted downward by 27% and 40%, respectively, from its rated values based the average field-measured deviations from rated efficiencies experienced by SS ASHPs previously field-tested in the Knoxville area (Munk et al. 2013). The results for this comparison are shown in Table 16. Since the hot water tank heat losses were not accounted for in the AS-IHP field test, they are also omitted from the baseline equipment efficiency (e.g., baseline WH COP of 1.0). This comparison assumes that the baseline ASHP meets the same total DH load as the prototype AS-IHP system. The table shows that the largest percentage savings come from WH, at 58% (1593 kWh). Note that the WH energy savings estimate (and that in Table 15) includes the impact of the 20-day period in January when the hot water load was zero, so this savings estimate is likely somewhat conservative. SC+DH and SH energy savings are estimated at 1812 kWh (45%) and 1836 kWh (26%), respectively. Estimated total annual savings for the AS-IHP vs. estimated baseline energy use at the Knoxville field-test site are ~38%. Heavy reliance on backup electric elements for SH and defrost tempering coupled with higher indoor blower energy usage vs. manufacturer's data were likely the major causes of the lower-than-expected SH performance of the AS-IHP field prototype system.

Table 16. AS-IHP system 2015–2016 energy savings vs. estimated baseline system performance at test site (based on 13 SEER ASHP field tests in 2011–2012)

Mode		AS-IHP	Baseline system estimated performance[a]	Percent Savings Over Baseline
Space Cooling + DH	Delivered (kWh)	9189	9189	
	Consumed (kWh)	2201	4013	45%
Space Heating	Delivered (kWh)	11,651	11,651	
	Consumed (kWh)	5225	7061	26%
Water Heating	COP	2.39	1	
	Delivered (kWh)	2739	2739	
	Consumed (kWh)	1146	2739	58%
Total	**Consumed (kWh)**	**8572**	**13,813**	**38%**

[a]Estimated per average measured performance of two 13 SEER ASHPs tested in the Knoxville area in 2011–2012; baseline WH performance assumed equal to that in Table 15.

7. FURTHER COMMERCIAL PRODUCT DEVELOPMENT PLANS

Further commercial development of this AS-IHP concept or the WH/DH module is currently a low priority for Lennox. Their available resources are focused on dealing with upcoming changes anticipated in the efficiency rules and testing requirements as well as an anticipated A2L refrigerant phase-in later this decade. The WH/DH will not be part of their product plan in the near future due to the current number of products they already have in development. The team is exploring the possibility of engaging with another company to manufacture the WH/DH. Lennox may be willing to license the technology.

8. CONCLUSIONS

Between October 2007 and September 2017, ORNL and Lennox engaged in a CRADA to develop an AS-IHP system for the US residential market. The Lennox AS-IHP concept consisted of a high-efficiency ASHP for SH/SC services and a separate heat pump WH/DH module for domestic WH/DH services. A key feature of this system approach with the separate WH/DH is the capability to pretreat (i.e., dehumidify) ventilation air and dedicated whole-house DH independent of the ASHP. Two generations of laboratory-prototype WH/DH units were designed, fabricated, and lab tested. Performance maps for the system were developed using the latest research version of the DOE/ORNL HPDM, as calibrated against the lab test data. These maps were the input to the TRNSYS system to predict annual performance relative to a baseline suite of equipment meeting minimum efficiency standards in effect in 2006 (combination of SEER 13 ASHP and electric resistance water heater with EF of 0.9). Predicted total annual energy savings, based on use of a two-speed ASHP and the second-generation WH/DH prototype for the AS-IHP—while providing space conditioning and WH for a tight, well insulated (i.e., nZEH-ready) 2600 ft^2 (242 m^2) house at 3 US locations with relative high DH loads—ranged from 33 to 36%, averaging 35%, relative to the baseline system (The lowest savings were realized at the cold-climate Chicago location.) Predicted energy use for WH was reduced by about 50 to 60% relative to resistance WH.

Based on the lab prototype test and results of analyses, Lennox designed and fabricated a field-test prototype WH/DH. The WH/DH prototype, together with a VS ASHP was installed in a 2400 ft^2 (223 m^2) house in Knoxville, TN and field tested from August 2015 to October 2016. Further field testing of

the WH/DH unit continued through May 2017 to evaluate several design changes intended to improve DH performance. For the 2015–2016 AS-IHP system test period, overall space conditioning efficiencies were 4.72 for SC) and 2.23 for SH. For WH, the overall average COP was 2.75 for the WH/DH unit only and was 2.19 for the total system including COP degradations due to (1) heat losses of ~10% from the connecting lines between WH/DH and tank, (2) heat losses of ~8% from the water tank, and backup electric heat usage of ~3%. The WH COP was also negatively impacted by a 20-day period in January 2016 when there were no hot water draws due to a control issue. Overall, the DH efficiency, including only months with significant run hours in DH mode, was 1.7 l/kWh; monthly averages ranged from 1.5 to 2.1.

Based on the demonstrated field performance of the AS-IHP prototype and estimated performance of a baseline system operating under the same loads and weather conditions, a bin analysis estimated that the prototype would achieve ~30% energy savings relative to the minimum efficiency suite. The estimated WH savings were ~60%, and SC mode savings were >30%. Estimated SH savings were only about 10% due to the atypically high heating load; zone control issues also played a part in reducing the expected heating performance. A secondary comparison based on prior field tests of two baseline 13 SEER ASHPs in another house with more typical heating-to-cooling-load ratios in the same area indicated ~40% overall energy savings for the AS-IHP (~60% WH savings, ~45% SC savings, and ~25% SH savings).

9. REFERENCES

Air-Conditioning, Heating, and Refrigeration Institute (AHRI). *2008 Standard for Performance Rating of Unitary Air-Conditioning & Air-Source Heat Pump Equipment.* AHRI 210/240. Arlington, VA: AHRI, 2008.

AHRI. Directory of Certified Product Performance. Accessed September 30, 2016. https://www.ahridirectory.org.

ANSI/Association of Home Appliance Manufacturers (AHAM). *Dehumidifiers*. DH-1 2008. Washington, DC: AHAM, 2008.

American Society of Heating, Refrigerating and Air-Conditioning Engineers (ASHRAE). *Ventilation and Acceptable Indoor Air Quality in Low-Rise Residential Buildings*. ASHRAE Standard 62.2-2007. Atlanta: ASHRAE, 2007.

ASHRAE. *ASHRAE Handbook: Fundamentals*. Atlanta: ASHRAE, 2013.

Baxter, V. D., C. K. Rice, J. D. Munk, M. R. Ally, and B. Shen. *Advanced Variable Speed Air-Source Integrated Heat Pump (AS-IHP) Development - CRADA Final Report*. ORNL/TM-2015/525, September 2015.

Code of Federal Regulations, US. "Uniform Test Methods for Measuring the Energy Consumption of Water Heaters." *Code of Federal Regulations*, title 10, chap. II, vol. 3, part 430, subpart B, appendix E. 2010.

Dobos, A. P. *PVWatts Version 1 Technical Reference*, Technical Report NREL/TP-6A20-60272, National Renewable Energy Laboratory (NREL), October 2013. http://www.nrel.gov/docs/fy14osti/60272.pdf.

Department of Energy, US (DOE). *Building Science-Based Climate Maps*. PNNL-SA-90570. January 2013. http://apps1.eere.energy.gov/buildings/publications/pdfs/building_america/-4_3a_ba_innov_buildingscienceclimatemaps_011713.pdf.

DOE. *EnergyPlus Version 8.6 Documentation: Engineering Reference*. September 30, 2016. https://energyplus.net/sites/all/modules/custom/nrel_custom/pdfs/pdfs_v8.6.0/EngineeringReference.pdf.

DOE/BTO Building America Program. Building America Analysis Spreadsheets: DHW Event Schedule Generator. Last accessed on September 24, 2015. http://energy.gov/eere/buildings/-building-america-analysis-spreadsheets.

Energy Star 2012. ENERGY STAR® Program Requirements for Dehumidifiers, Version 3.0. US Environmental Protection Agency Energy Star Program.

Energy Star 2013. ENERGY STAR® Program Requirements for Residential Water Heaters, Version 2.0, July 1. US Environmental Protection Agency Energy Star Program.

Energy Star 2015. ENERGY STAR® Program Requirements for Residential Water Heaters, Version 3.1, April 16. US Environmental Protection Agency Energy Star Program. https://www.energystar.gov/products/water_heaters/heat_pump_water_heaters

Energy Star 2016. ENERGY STAR® Program Requirements for Dehumidifiers, Version 4.0, October 25. US Environmental Protection Agency Energy Star Program. https://www.energystar.gov/products/appliances/dehumidifiers/key_efficiency_criteria

Hendron, R. and C. Engebrecht. *Building America House Simulation Protocols*. NREL Report: TP-550-49426, October 2010.

Hendron, R., J. Burch, and G. Barker. *Tool for Generating Realistic Residential Hot Water Event Schedules*. Preprint. United States: s.n., 2010. NREL/CP-550-47685.

Lennox Industries Inc. "Lennox Engineering Data, Heat Pump Outdoor Units, XP19." Bulletin No. 210415, March 2009a.

Lennox Industries Inc. "Lennox Engineering Data, Heat Pump Outdoor Units, XP19, Expanded Ratings Tables", Bulletin No. 210415R, April 2009b.

Lennox Industries Inc. "SunSource® Home Energy System Product Specifications." Publication #210664, September 2013a.

Lennox Industries Inc. "SunSource® Home Energy System Application and Design Guidelines." Publication #CORP1312-L2, July 2013b.

Lennox Industries Inc. "Lennox XP-25 2 to 5 Ton Heat Pump Product Specifications," Bulletin 210659, May 2014.

Munk, J. D., C. Halford, and R. Jackson. *Component and System Level Research of Variable-Capacity Heat Pumps.* ORNL/TM-2013/36, Oak Ridge National Laboratory, June 2013.

Munk, J. D., V. D. Baxter, A. C. Gehl, M. R. Ally, B. Shen, C. K. Rice, and R. B. Uselton. "Prototype Air-Source Integrated Heat Pump Field Evaluation Results." Paper O.1.4.1 in Proceedings of the 12th IEA Heat Pump Conference, Rotterdam, The Netherlands, May 15–18, 2017.

Murphy, R.W., V. D. Baxter, C. K. Rice, and W. G. Craddick. *Air-Source Integrated Heat Pump for Near Zero Energy Houses: Technology Status Report*. ORNL/TM-2007/112, December 2007.

National Oceanic and Atmospheric Administration (NOAA) *NOAA Online Weather Data*. Accessed August 3, 2015, and August 14, 2015. http://w2.weather.gov/climate/xmacis.php?wfo=mrx.

NOAA. *NOAA Online Weather Data*. Accessed December 22, 2016. http://w2.weather.gov/climate/xmacis.php?wfo=mrx

NREL. BEopt version 2.4.0.1. Golden, CO: NREL, 2015.

Rice, C. K. "Benchmark Performance Analysis of an ECM-Modulated Air-to-Air Heat Pump with a Reciprocating Compressor." *ASHRAE Transactions* vol. 98, part 1, 1992.

Rice, C. K. and W. L. Jackson 2005. DOE/ORNL Heat Pump Design Model on the Web, Mark VII Version. Last updated August 2, 2013. http://www.ornl.gov/~wlj/hpdm/MarkVII.shtml.

Rice, C. K., B. Shen, V. D. Baxter, S. S. Shrestha, and R. B. Uselton. "Development of an Air-Source Heat Pump Integrated with a Water Heating/Dehumidification Module." *Conference Proceedings of the 11th IEA Heat Pump Conference*, Montréal (Québec), Canada, May 12-16.

Risser, R. "Driving Innovation, Speeding Adoption, Scaling Savings – an Overview of the DOE Building Technologies Office," Presented at the 2016 DOE/BTO Peer Review Meeting, Washington, DC, April 4, 2016. https://energy.gov/eere/buildings/building-technologies-office-2016-peer-review-0

Shen, B., O. A. Abdelaziz, and C. K. Rice. "Auto-Calibration and Control Strategy Determination for a Variable-Speed Heat Pump Water Heater Using Optimization," *International Journal of HVAC&R* vol. 18, no. 5, October 2012.

Solar Energy Laboratory, University of Wisconsin, TRANSSOLAR Energietechnik, CSTB—Centre, Scientifique et Technique du Bâtiment, and TESS—Thermal Energy System Specialists. TRNSYS 16: a TRaNsient SYstem Simulation Program, version 16.01.0000.

Uselton, R. *Dedicated Dehumidifier and Water Heater*. United States Patent Application Publication, Pub. No. US 2012/0047930 A1, March 1, 2012.

Uselton, R. Dedicated Dehumidifier and Water Heater, United States Patent 8,689,574 B2, April 1, 2014.

APPENDIX A. INVENTION DISCLOSURES FILED UNDER CRADA WORK PROGRAM

This appendix lists invention disclosures resulting from work done under this CRADA project.

1. Joint disclosures by Lennox and ORNL – none

2. Disclosures by ORNL – Invention Disclosure - "Condensate Removal Aid for Heat Exchangers," October 2015, Docket Number 201503585

3. Disclosures by Lennox – patent titled "Dedicated Dehumidifier and Water Heater" (patent No.: US 2014/8,689,574 B2) was awarded by US patent office on April 1, 2014.